



Forschungszentrum Karlsruhe
Technik und Umwelt

Wissenschaftliche Berichte
FZKA 5764

**Safety and Environmental
Impact of the Dual Coolant
Blanket Concept**

SEAL Subtask 6.2, Final Report

**K. Kleefeldt, F. Dammel, K. Gabel,
T. Jordan, I. Schmuck**

**Institut für Reaktorsicherheit
Projekt Kernfusion**

März 1996

**Forschungszentrum Karlsruhe
Technik und Umwelt**

Wissenschaftliche Berichte

FZKA 5764

**Safety and Environmental Impact
of the Dual Coolant Blanket Concept**

(SEAL Subtask 6.2, Final Report)

K. Kleefeldt, F. Dammel, K. Gabel, T. Jordan, I. Schmuck

Institut für Reaktorsicherheit

Projekt Kernfusion

Forschungszentrum Karlsruhe GmbH, Karlsruhe

1996

Als Manuskript gedruckt
Für diesen Bericht behalten wir uns alle Rechte vor

Forschungszentrum Karlsruhe GmbH
Postfach 3640, 76021 Karlsruhe

ISSN 0947-8620

Note:

This work has been performed in the framework of the
Nuclear Fusion Project of the Forschungszentrum Karlsruhe GmbH
and is supported by the European Communities
within the European Fusion Technology Programme.

Abstract

The European Union has been engaged since 1989 in a programme to develop tritium breeding blankets for application in a fusion power reactor. There are four concepts under development, namely two of the solid breeder type and two of the liquid breeder type. At the Forschungszentrum Karlsruhe one blanket concept of each line has been pursued so far with the so-called dual coolant type representing the liquid breeder line. In the dual coolant concept the breeder material (Pb-17Li) is circulated to external heat exchangers to carry away the bulk of the generated heat and to extract the tritium. Additionally, the heavily loaded first wall is cooled by high pressure helium gas.

The safety and environmental impact of the dual coolant blanket concept has been assessed as part of the blanket concept selection exercise, a European concerted action, aiming at selecting the two most promising concepts for further development. The topics investigated are: (a) blanket materials and toxic materials inventory, (b) energy sources for mobilisation, (c) fault tolerance, (d) tritium and activation products release, and (e) waste generation and management. No insurmountable safety problems have been identified for the dual coolant blanket. The results of the assessment are described in this report. The information collected is also intended to serve as input to the EU "Safety and Environmental Assessment of Fusion long-term Programme" (SEAL). The unresolved issues pertaining to the dual coolant blanket which would need further investigations in future programmes are outlined herein.

Gesichtspunkte der Sicherheit und Umwelteinflüsse des Flüssigmetall-Blankets vom Typ 'Dual Coolant' für einen DEMO Reaktor

KURZFASSUNG

Im Forschungsprogramm der Europäischen Union werden seit 1989 tritiumbrütende Blankets für den Einsatz in Fusionsreaktoren entwickelt. Bislang befanden sich vier Varianten in der näheren Untersuchung, nämlich je zwei Varianten mit festem und flüssigem Brutstoff. Im Forschungszentrum Karlsruhe wurden beide Linien verfolgt. Für die Linie mit flüssigem Brutstoff ist es das sogenannte Dual-Coolant-Konzept (englisch für zwei Kühlmittel). In ihm wird der flüssige Brutstoff, die eutektische Verbindung Pb-17Li, zu externen Wärmetauschern geführt, um sowohl die erzeugte Wärme als auch das erbrütete Tritium abzuführen. Die sehr hochbelastete erste Wand wird hingegen mit gasförmigem Helium gekühlt.

Die Sicherheits- und Umwelteinflüsse des Dual-Coolant-Konzeptes wurden im Rahmen des europäischen Blanket-Auswahlverfahrens betrachtet, welches zum Ziel hatte, zwei der vier Varianten für die weitere Entwicklung auszuwählen. Die dabei behandelten Themen waren a) Art und Mengen der beteiligten radiotoxischen Stoffe, b) Energieinhalte als mögliche Ursache für Aktivitätsfreisetzungen, c) Störfallverhalten, d) Freisetzung von Tritium und anderen Aktivitätsprodukten und e) Erzeugung radioaktiver Abfälle. Für das Dual-Coolant-Konzept wurden wie bei den anderen Varianten keine schwerwiegenden Sicherheitsprobleme erkannt. Die Ergebnisse zu den untersuchten Themen werden im Bericht dargestellt. Am Schluß werden einige Aspekte herausgestellt, die noch weiterer Analysen bedürfen. Das Datenmaterial dient auch als Beitrag zu einem laufenden Vierjahresprogramm der EU über Sicherheit und Umwelteinflüsse der Fusionstechnologie (SEAL).

Contents

1.0 Introduction	1
2.0 Blanket Materials and Toxic Materials Inventory	3
2.1 Volumes and Volume Fractions in the Blanket Segments	3
2.2 Coolant Inventories	3
2.2.1 Inventories in Piping	4
2.2.2 Inventories in Components	6
2.2.3 Summary of Coolant Inventories	6
2.3 Toxic Inventories	6
2.3.1 Tritium Inventory	7
2.3.2 Activation Products Inventory	8
2.3.2.1 Activation of Pb-17Li	8
2.3.2.2 Activation of Structural Material	9
2.3.2.3 Activation of Insulating Layers	10
3.0 Energy Sources for Mobilization	13
3.1 Energy Liberated during Plasma Disruptions	13
3.2 Energy due to Delayed Plasma Shutdown	13
3.3 Decay Heat	13
3.4 Work Potential of Helium Coolant	15
3.5 Exothermic Chemical Reactions Review	16
3.5.1 Pb-17Li-Water Reactions	16
3.5.2 Pb-17Li-Air Reactions	17
3.5.3 Pb-17Li-Nitrogen Reactions	18
3.5.4 Pb-17Li-Concrete Reactions	18
4.0 Fault Tolerance	19
4.1 Behavior during Electromagnetic Transients	19
4.2 LOCA Temperature Transients	20
4.2.1 LOCA in one First Wall Helium Subsystem	20
4.2.2 LOCA in the Pb-17Li Circuit	20
4.2.3 LOCA in the NaK Circuit	21
4.3 Temperature Distribution during Handling	21
4.3.1 Temperature Distribution in Gas-filled Segments	21
4.3.2 Temperature Distribution in Pb-17Li-filled Segments	23
5.0 Tritium and Activation Products Release	25
5.1 Release during Normal Operation	25
5.2 Tritium Release in Accidental Situations	25
5.3 Activation Products Release in the case of a Pb-17Li LOCA	27

6.0 Waste Generation and Management	31
7.0 Summary and Conclusions	33
7.1 Summary of Results	33
7.2 Conclusions	34
8.0 References	37
9.0 Tables	39
10.0 Figures	53
Appendix A. Volumes and Volume Fractions	73
A.1 Results	73
A.2 Detailed Results	80
A.2.1 Outboard Blanket (central part)	81
A.2.2 Outboard Blanket (top part)	82
A.2.3 Inboard Blanket (central part)	83
A.2.4 Inboard Blanket (top part)	84
A.2.5 Inboard Blanket (bottom part)	84

Tables

1.	Thermal power and redundancy factors for primary cooling circuits	39
2.	Geometrical data of blanket Pb-17Li circuit components (outboard)	40
3.	Geometrical data of blanket Pb-17Li circuit components (inboard)	41
4.	Geometrical data of first wall helium circuit components (outboard)	42
5.	Geometrical data of first wall helium circuit components (inboard)	43
6.	Coolant inventory in primary circuits (summary)	44
7.	Tritium inventory in blanket and related systems	44
8.	Specific and total activity in Pb-17Li	45
9.	Specific and total activity in structural material	46
10.	Specific and total activity in Pb-17Li after various decay times	47
11.	Total and mixed mean specific activity in different regions of the blanket structure	47
12.	Activation and dose rate of aluminum in MANET	48
13.	Energy sources for mobilization	49
14.	Afterheat power density and total afterheat in Pb-17Li	50
15.	Afterheat power density and total afterheat in structural material	51
16.	Early and chronic dose for accidental tritium release from fluids	52
17.	The twelve largest contributors to the early dose in case of a Pb-17Li spill	52
18.	Radioactive waste of the blanket system	52
19.	Main dimensions of the DEMO blanket	73
20.	Volume of the dual coolant blanket	74
21.	Volume fractions of steel and Pb-17Li in different blanket parts	75
22.	Steel volumes in the different blanket parts	75
23.	Definition of variables used in Appendix A	80

Figures

1.	DEMO cross section of the dual coolant blanket	54
2.	Cross sectional view of the outboard blanket segment at midplane	55
3.	Cross sectional view of the inboard blanket segment at midplane	56
4.	Perspective view of the dual coolant blanket (outboard)	57
5.	Schematic diagram of a Pb-17Li cooling circuit for the outboard blanket	58
6.	Tritium concentration in MANET in the outboard blanket	59
7.	Activation parameters of Pb-17Li of the dual coolant blanket	60
8.	Activity dominating nuclides in Pb-17Li vs. decay time	61
9.	Elemental composition of Pb-17Li in outboard front channels	62
10.	Elemental composition of MANET in the first wall	63
11.	Adiabatic temperature rise of blanket materials due to decay heat	64
12.	Depressurization of an outboard cooling subsystems	65
13.	Distribution of von-Mises stresses with fixed back plate during a disruption	66
14.	Maximum von-Mises stress with fixed back plate during a disruption	67
15.	Temperature history during a LOCA at selected points of the first wall	68
16.	Radial temperature profiles in the structure of the outboard blanket segment during handling	69
17.	Radial temperature profiles in the structure of the outboard blanket segment during handling	70
18.	Toroidal temperature profiles in the structure of the outboard blanket segment during handling	71
19.	Temperature distribution in the outboard blanket segment during handling	72
20.	Volume histogram of steel for radial layers in the outboard blanket	76
21.	Volume histogram of Pb-17Li for radial layers in the outboard blanket	77
22.	Volume histogram of steel for radial layers in the inboard blanket	78
23.	Volume histogram of Pb-17Li for radial layers in the inboard blanket	79

1.0 Introduction

The European Union has been engaged since 1989 in a programme to develop tritium breeding blankets for application in a fusion power reactor. There are four concepts under development. Two of these blanket concepts use lithium ceramics as breeder material (solid breeder blankets), the other two concepts employ a eutectic lead-lithium alloy as breeder material (liquid metal breeder blankets).

At the Forschungszentrum Karlsruhe one blanket concept of each line has been pursued so far, i.e., the breeder-outside-tube solid breeder blanket [1], representing the solid breeder line, and the so-called dual coolant blanket, representing the liquid breeder line. In the dual coolant blanket concept, the breeder material (Pb-17Li) is circulated to external heat exchangers to carry away the bulk of the generated heat and to extract the tritium produced in the liquid metal. The heavily loaded first wall, instead, where a liquid metal flow is hard to achieve due to MHD flow resistance, is cooled by an extra high pressure helium gas flow. The use of two coolants gave the the concept the name.

The current state of development of the dual coolant blanket concept has most recently been documented in a comprehensive status report [2]. The present report is an extended version of the contribution to the status report, dealing with the safety aspects of the dual coolant blanket for a DEMO reactor. It covers the topics (a) blanket materials and toxic materials inventory, (b) energy sources for mobilization, (c) fault tolerance, (d) tritium and activation products release, and (e) waste generation and management. This work was performed in the frame of the blanket concept selection exercise (BCSE), aiming at selecting two of the four concepts for further development. The BCSE was a joint effort among the associations developing the four concepts, and industry, under the auspices of the European Commission.

In the frame of the safety and environmental assessment of fusion power long-term programme (SEAL) a task (SEAL 6) is being performed on "blanket safety analysis for the four European blanket concepts" in support of BCSE. The task is coordinated by UKAEA. FZK agreed to provide input information under subtask SEAL 6.2 "Input for the dual coolant blanket and ceramic breeder blanket". Besides the above mentioned status report character, this report has been extended to contain the necessary information needed in SEAL 6 as far as the dual coolant concept is concerned. (For the ceramic breeder blanket concept, this is done in [3].) In particular it contains supplemental data and references in the fields of materials distribution in the blanket segments, cooling circuitry, elemental composition of blanket materials, activation and afterheat data in different blanket regions, tritium and activation products profiles, and temperature profiles during handling. Most of the afterheat and activation data are derived from the neutronics analyses documented in [4] and [5].

2.0 Blanket Materials and Toxic Materials Inventory

2.1 Volumes and Volume Fractions in the Blanket Segments

The total volume in different parts of the dual coolant blanket and the volume fractions of steel, Pb-17Li, helium and void have been calculated for both outboard and inboard blanket. The basis for the assessment is the vertical cross section for the DEMO reactor (Figure 1 on page 54) and the midplane cross sections of inboard and outboard blanket segments (Figure 2 on page 55 and Figure 3 on page 56) taken from [6].

Note: The outboard cross sectional view differs slightly from the most recent design documented in [7], e.g., in respect to the back plate thickness of 246 mm in the new design versus 200 mm used here.

The main dimensions used in the calculations are described in Appendix A on page 73 together with detailed results for volumes of steel, Pb-17Li, helium, and void in radial layers of different blanket parts, i.e, outboard central, outboard top, inboard central, inboard top, and inboard bottom. To ease the discussion of radial effects, three radial zones have been defined, namely first wall, breeding zone, and shield region (essentially the removable back plate) as depicted in Figure 3 on page 56 and Figure 4 on page 57. Hence, the manifolding region containing the helium channels next to the back plate is assigned here to the breeding zone. The computed volumes for the blanket parts (outboard central and top part, and inboard central, top, and bottom part behind the divertors) are listed in Table 20 on page 74. The total blanket volume results to about 1020 m^3 with volume fractions of 40/41/16/3 percent for steel/Pb-17Li/He/void, respectively.

Figure 20 and Figure 21 in Appendix A illustrate the radial volume distribution of steel and Pb-17Li, respectively, for the central part of the outboard blanket between the poloidal angles $\phi = -52^\circ$ to $\phi = +48^\circ$.

Similarly, Figure 22 and Figure 23 represent the radial volume distribution of steel and Pb-17Li for the cylindrical part of the inboard blanket with a total length of 800 cm.

For more details see Appendix A on page 73.

2.2 Coolant Inventories

Coolant inventories in the primary cooling circuits of the dual coolant blanket have been calculated for the piping system added on estimates for other components like steam generators, pumps, purification systems, and expansion vessels.

The loop arrangements and thermal power per loop have been taken as described in 2.2.1 on page 4, accounting for redundancies in the primary circuit layout. This leads to larger power capacities as compared to the nominal power to be removed from the blanket segments. Hence, the loops (except for the feeders between the ring collectors and the blanket segments) become substantially larger than they would be required for the nominal power capacity. Table 1 on page 39 gives an overview of the nominal thermal power to be removed by Pb-17Li and helium from the inboard and outboard blanket segments. It also shows the redundancy factors discussed below and the required power capacities of the external loops, which result from equation 1. As a consequence of this redundant circuit layout, the external loops (including the ring collectors and the components) have to be dimensioned for the case that one circuit of the subsystem fails (Table 1 on page 39).

Note: The redundancy factor results from the systems layout and is expressed as follows: All subsystems consisting of n circuits ($n = 2, 3, \text{ or } 4$) are designed in a 2-out-of- n redundancy, meaning that at least two circuits of a subsystem must fail for the plant to be unavailable. For instance, for a 2-out-of-3 subsystem to be unavailable, 2 circuits must fail. Hence, it is available, if 1 circuit fails, in which case the remaining circuits have to take 1.5 (the redundancy factor) times the nominal power. In the same way the redundancy factor of 2 corresponds to a 2-out-of-2 subsystem, and the redundancy factor of 1.33 corresponds to a 2-out-of-4 subsystem.

The required power capacity per circuit (in the event that one circuit of a subsystem has failed or is in stand-by) has been calculated by use of the following equation. Note that, due to the redundancy, the overall installed power capacity of the cooling system (3120 MW) is 51 % larger than the nominal power to be removed from the blanket (2067 MW).

$$\text{Required power capacity per circuit} = \frac{P_{segment} n_{segment}}{n_{circuit}} f_{redundancy} \quad (1)$$

where

- $P_{segment}$ = thermal power per segment
- $n_{segment}$ = number of blanket segments
- $n_{circuit}$ = number of installed primary circuits
- $f_{redundancy}$ = redundancy factor (see Table 1 on page 39)

2.2.1 Inventories in Piping

For the **Pb-17Li circulation in the outboard blanket**, six circuits with steam generators, pumps, purification stations, and expansion vessels are foreseen as outlined in [8], serving the 48 outboard segments. Each three of such circuits are joined at the ring collectors to form two 2-out-of-3 Pb-17Li subsystems, each of which supplies the coolant for one 180 degree sector of the torus. If all circuits are intact, one cir-

cuit per subsystem is in stand-by or, alternatively, all three circuits per subsystem are operated at reduced power.

Likewise, for the **Pb-17Li circulation in the inboard blanket**, four circuits with steam generators, pumps, purification stations, and expansion vessels are foreseen, serving the 32 inboard segments. They are joined at the ring collectors to form one 2-out-of-4 redundancy. If all circuits are intact, one circuit is in stand-by or, alternatively, all four circuits are operated at reduced power.

Pipe lengths for the hot leg, cold leg, ring collectors, and feeders have been estimated based on a loop arrangement as schematically shown in Figure 5 on page 58 and listed in Table 2 on page 40 and Table 3 on page 41. The lengths are of the order of 116 m per outboard loop (140 m per inboard loop), not accounting for parallel branches. Pipe diameters result from the flow rates necessary to remove 277 MW thermal power for the outboard circuits and 147 MW for the inboard circuits, respectively, with inlet/outlet temperatures of 275/425 °C and an assumed flow velocity of the Pb-17Li of 1 m/s. Typical pipe dimensions for the outboard/inboard circuits are 1.15m/0.83m for the main loops, 0.94m/0.72m for the ring collectors, and 0.33m/0.25m for the feeders.

Concerning the **helium loops for the outboard first wall cooling**, the loop arrangement is similar to that of the Pb-17Li system. Again, six main circuits with steam generators, circulators and clean-up systems serve the first wall of the 48 outboard blanket segments. For redundancy purposes each three of such circuits are joined at the collectors to form two 2-out-of-3 helium cooling subsystems. In contrast to the Pb-17Li system each of the first wall cooling subsystems serves the full 360 degree sector of the torus in two parallel streams, requiring two inlet and two outlet helium feeders per segment. If all circuits are intact, one circuit per subsystem is in stand-by, or alternatively, all three circuits are operated at reduced power. Pipe lengths are assumed to be 172 m per outboard loop, not accounting for parallel branches. Counting the 32 parallel feeders (16 inlet and 16 outlet) to the outboard segments would result in a total pipe length of 652 m per circuit (Table 4 on page 42). Pipe diameters in the different pipe sections result from the flow rates necessary to remove 83 MW per circuit, given inlet/outlet temperatures of 250/350 °C and a system pressure of 8 MPa with an assumed flow velocity of 60 m/s. Typical pipe diameters are 0.76 m for the hot leg, 0.7 m for the cold leg, 0.6 m for the ring collectors, and 0.15 m for the feeders (Table 4 on page 42).

Finally, the **helium loops for the inboard first wall cooling** are also similar to those of the Pb-17Li system. Four main circuits are foreseen, serving the first wall of the 32 inboard blanket segments. For redundancy purposes each two of such circuits are joined at the collectors to form two 2-out-of-2 helium cooling subsystems. As for the outboard each of the two first wall cooling subsystems serves the full 360 degree sector of the torus in two parallel streams. If all circuits are intact, one circuit per

subsystem is in stand-by, or, alternatively, the two circuits are operated at reduced power. Pipe lengths are assumed to be similar as for the outboard except for the ring collector length and feeder lengths, resulting in a total length of 220 m per inboard loop, not accounting for parallel branches. Typical pipe diameters are 0.8 m for the hot leg, 0.73 m for the cold leg, 0.55 m for the ring collectors, and 0.14 m for the feeders (Table 5 on page 43).

2.2.2 Inventories in Components

The assumed coolant inventories in the circuit components are rough estimates. The dominating components are the steam generators, for which a first layout has been performed [2]. Based on the dimensions reported, the Pb-17Li inventories result to approximately $22.5 m^3$ and $11.3 m^3$ for the 277 MW and 147 MW steam generators in the outboard and inboard circuits, respectively. The helium inventory in the 83 MW steam generator for the outboard first wall cooling circuit would be approximately $9.4 m^3$ and in the 93 MW steam generator for the inboard first wall cooling circuit would be approximately $10.5 m^3$. Helium and Pb-17Li inventories in the blanket segments are evaluated in 2.1 on page 3.

2.2.3 Summary of Coolant Inventories

Coolant inventories in primary cooling circuits (excluding ancillaries, like e.g., storage tanks) are summarized in Table 6 on page 44 for the Pb-17Li and helium circuits. A more detailed representation is given in Table 2 on page 40 to Table 5 on page 43. The total Pb-17Li inventory amounts to $14.8 \times 10^6 kg$ ($1571 m^3$) and the total helium inventory amounts to 6293 kg ($969 m^3$). Also given in Table 6 are the data for the subsystems. This is important in assessing leak rates in case of pipe rupture, without the capability to isolate the failed circuit in time. Thus, one Pb-17Li outboard cooling subsystem with three circuits contains $569 m^3$ of Pb-17Li. The inboard cooling subsystem with four circuits contains $433 m^3$ of Pb-17Li. Only part of this can be drained by gravity in case of a pipe rupture or blanket segment failure. The respective first wall cooling subsystems carry $298 m^3$ (1934 kg) of helium to the outboard and $187 m^3$ (1213 kg) to the inboard. Most of the coolant inventory is in the piping (53-60 %), only 18-22 % being in the blanket proper.

2.3 Toxic Inventories

Radioactive inventories in the different regions of the blanket (first wall, breeding zone and shield region) as well as in the cooling systems have been assessed in two categories, i.e., tritium and other activation products. No intentional chemical toxins, like beryllium, are foreseen in the dual coolant blanket concept. Inventories are discussed for the whole blanket system, if not otherwise stated.

2.3.1 Tritium Inventory

The tritium inventory in the breeder (Pb-17Li) is determined by the recovery process (permeation through the outer wall of the steam generator tubes into the NaK circuit) as outlined in section 7.1 of [2]. Given an equilibrium partial pressure of 147 Pa and a Pb-17Li mass of 15×10^6 kg (see 2.2.3), the total tritium inventory in the breeder (excluding the recovery system) amounts to 57 g. In one coolant subsystem for the outboard consisting of 3 circuits the tritium inventory is 21 g. In the subsystem for the inboard consisting of four circuits the tritium inventory is 16 g.

A considerable amount of tritium ($\simeq 4$ g/d) will permeate into the helium coolant passing the first wall channels, if no credit is taken of any permeation barrier, e.g. the Al_2O_3 electrical insulation at the steel/Pb-17Li interface. This tritium is assumed to be permanently removed in a tritium extraction plant, so that the tritium concentration in the helium can be kept low, say < 1 wppm [9], corresponding to a total tritium inventory of < 6.3 g in 6300 kg of helium. This is partitioned into four subsystems as outlined in 2.2.1 on page 4.

The tritium inventory in the NaK circuits has been derived in [2] to be 0.38 g in a total of 4.1×10^4 kg of NaK. Each steam generator has an independent NaK system with cold traps. Therefore, the maximum tritium inventory occurring in a single NaK subsystem for the outboard is about 0.04 g. This is small compared to the tritium trapped in the cold traps (see below).

Control of the tritium losses to the steam circuit is a common critical issue, requiring permeation barriers, a low tritium partial pressure in the NaK circuits (or in the first wall helium coolant, respectively) and control of the water/steam circuit chemistry. Estimates revealed for the NaK/Water tubes in the steam generators a tritium permeation rate of 0.12 g/d (1200 Ci/d) for ferritic steel (for 10 steam generators) without any permeation barrier. Thus, barrier factors of the order of 120 need to be achieved in order to reduce the losses to 10 Ci/d. The first wall helium cooling system has to cope with similar problems, and a tritium loss of another 10 Ci/d seems to be feasible [10]. The total tritium losses of 20 Ci/d (0.002 g/d) would accumulate to 1.7 g of tritium in the entire water/steam system after 20000 h of operation. This is considered to be acceptable (compare [8], [10]).

The tritium inventory in the recovery system is dominated by the inventory in the cold traps and amounts to about 15 g for the cold traps in one NaK circuit for an outboard steam generator (see section 7.1 of [2]) and approximately 100 g for all cold traps.

The tritium build-up in the structural material after 20000 h has been evaluated for the outboard blanket [5]. The poloidally averaged concentration as a function of radius falls off linearly in a semi-logarithmic scale by four orders of magnitude, i.e., from 3×10^{-5} g per kg of MANET in the first wall to 3×10^{-9} g per kg of MANET

in the shield region. The tritium profile (Figure 6 on page 59) weighted with the corresponding mass distribution of steel (Figure 20 on page 76) results in a total tritium inventory of 2.2 g in the central part of the outboard blanket (excluding the top part), that is about 1.3 g in the first wall, 0.9 g in the steel of the breeding zone, and only 0.003 g in the shield region.

For the top part of the outboard blanket as well as for the inboard blanket the tritium inventory has not been elaborated. Due to the small amount it is assumed that this is of the same order of magnitude as the inventory in the central part of the outboard, leading to a total tritium inventory in the whole blanket structure of $\simeq 4.4$ g ($\simeq 2.6$ g in the first wall, 1.8 g in the breeding zone, and 0.006 g in the shield region). However, this does not account for the tritium implanted in the first wall from the plasma. This may be much higher and is currently assumed to range between 3 g and 300 g. It should also be noted that the solubility of tritium in MANET at a partial pressure equal to that in the Pb-17Li ($\simeq 150$ Pa) is of the order of 10^{-5} g per kg of MANET at 350 °C. This is in the same range as the build-up in the first wall discussed above but is much higher than the build-up in the breeding zone and shield region. Nevertheless, a substantial take-up of tritium from the Pb-17Li will be impaired by the electrical insulation layer.

An overview of the mass and tritium inventory in the breeder material, coolants and in the major radial zones of the structural material is given in Table 7 on page 44.

2.3.2 Activation Products Inventory

2.3.2.1 Activation of Pb-17Li

The specific activity in Pb-17Li has been assessed in the neutronics analysis [5]. For example, the specific activity in the outboard blanket (averaged over the liquid metal in the central plus the top blanket part) after decay times of 0 s, 1 d, and 1 year amounts to 3.3×10^{13} , 7.0×10^{11} , and 3.0×10^9 Bq/kg, respectively. Corresponding values obtained for the inboard are almost the same (Table 8 on page 45). Please note that the specific activity shortly after shutdown is dominated by the short-lived Pb isotopes, in particular Pb-207 with a half life of 0.8 s, so that after a few seconds the initial values are already reduced by one order of magnitude, and after about 1 day, by another order of magnitude.

In the neutronics calculations it was assumed that the Pb-17Li remained stationary in the blanket for the 20000 hours of operation. Given the liquid metal inventory in the blanket proper (excluding external circuits) of about 900,000 kg inboard and 3,100,000 kg outboard would result in a total activity in the Pb-17Li after decay times of 0 s, 1 d, 1 y of 1.3×10^{20} , 2.8×10^{18} , and 1.2×10^{16} Bq, respectively (see Table 8 on page 45 for longer decay times).

Due to the circulation the specific activity will be altered. As a first approach it is assumed here that the specific activity is diluted by the ratio of the total Pb-17Li inventory in the cooling circuits to the inventory in the blanket itself. This ratio (and hence the dilution factor) is 3.5 for the outboard cooling system and 4.7 for the inboard cooling system. The total radioactive inventory, on the other hand, is assumed to be unchanged. Table 10 on page 47 summarises the averaged specific and total activity in Pb-17Li in the inboard and outboard blanket for various decay times as evaluated from FISPACT calculations [5] and when considering a dilution in external circuits.

The time behavior of the activation parameters (specific activity, nuclear heat, γ -dose rate, ingestion dose, and inhalation dose) are plotted in Figure 7 on page 60 for the first channel row next to the first wall, reproduced from [4]. It can be seen that they run almost in parallel decreasing by seven orders of magnitude after 1000 to 10000 years.

The dominating nuclides in Pb-17Li of the first channel row in terms of specific activity at various decay times can be seen from Figure 8 on page 61. In the short term (tens of seconds) Pb-207m dominates clearly before Pb-203 takes the lead for days and weeks. Then at 1 month Hg-203 comes up, followed by Tl-204 which then leads for several decades of decay. In the very long term, Pb-205 (and Ag-108m for several centuries) become dominating.

The elemental composition of the Pb-17Li after 20000 hours of operation in the first channel row is illustrated in Figure 9 on page 62. It shows the base materials being lithium (0.7 %) and lead (99.3 %), the impurities that have been defined for the DEMO blanket, i.e., Fe, Ni, Zn, Bi, Cd, Ag, and Sn, and the transmutation products. Of each element present in the material, two up to five neighbours in the periodic system to each side are produced. In particular the generation of Hg, Tl, Bi, and Po constituting high biological hazards is evident. They originate mostly from Pb and cannot be avoided.

2.3.2.2 Activation of Structural Material

The specific activity of the structural blanket material (MANET) as assessed in the neutronics analyses [4], [5] has been reformatted here with view to safety aspects. Average specific activities and total activities are deduced for major blanket regions (inboard, outboard), radial zones (first wall, breeding zone, shield region), and various decay times (0 s, 1 d, 1 y, 10 y, 500 y), see Table 9 on page 46.

For instance, the specific activity in the "first wall region midplane average outboard" after decay times of 0 s, 1 d, 1 y, and 10 years is, respectively, 6.6×10^{14} , 4.0×10^{14} , 2.4×10^{14} , and 2.0×10^{13} Bq/kg. It is the highest specific activity in the blanket. Corresponding numbers at the inboard blanket are about 10 % lower. In contrast to the activity in Pb-17Li the decay in MANET is very slow, i.e., only by a

factor of three within the first year. In radial direction the decrease is about one order of magnitude from the first wall to the breeding zone, and another order of magnitude from the breeding zone to the shield region. Typical radial profiles and decay curves are given in [5].

Looking at the poloidally averaged values of the specific activity in the same radial zones which combine the respective radial zones in the central and top part of the outboard blanket, and in the central plus top and bottom parts of the inboard blanket, one observes a reduction relative to the midplane values by typically a factor of 0.7 in the outboard and 0.4 in the inboard.

The poloidally averaged values have been used to compute the total activity in the corresponding blanket regions by weighting them with the mass inventory of MANET. Summing up over all blanket regions results in a total activity after 0 s, 1 d, 1 y, and 10 years of 7.5×10^{19} , 4.0×10^{19} , 2.2×10^{19} , and 1.8×10^{18} Bq, respectively, in a total steel mass of 3.1×10^6 kg (Table 9 on page 46).

The elemental composition of the MANET after 20000 hours of operation is illustrated in Figure 10 on page 63. It shows the base materials and alloying elements (Fe, Cr, Ni, V, Mo, Nb, C), the impurities that have been defined for the DEMO blanket, (Si, Mn, P, S, B, N, Al, Co, Cu, Zr), and the transmutation products. Of each element present in the material, two up to five neighbours in the periodic system to each side are produced. The dominating nuclides in terms of specific activity and γ -dose rate vary with the decay time and are summarised below:

- ^{55}Fe , ^{54}Mn dominate the activity in the 1 year range
- ^{63}Ni , ^{94}Nb , ^{93}Mo dominate the activity in the $10^2 - 10^5$ years range
- ^{99}Tc dominates the activity in the very long range
- ^{54}Mn dominates the γ -dose rate in the 1 year range
- ^{94}Nb dominates the γ -dose rate in the $10^2 - 10^5$ years range
- ^{94}Nb , ^{26}Al dominate the γ -dose rate in the very long range
- Mo adds in activity but does not show up in the γ -dose

To summarise the activity in MANET Table 11 on page 47 lists the total activities after a 10 year decay period in the first wall, breeding zone, and shield region (each one for inboard and outboard blanket) and the corresponding steel masses. This division is of interest for waste purposes.

2.3.2.3 Activation of Insulating Layers

The activation of the insulating layer (Al plus Al_2O_3) has not been elucidated but an estimation based on the effect of 500 wppm Al impurities in MANET is presented below and quantified in Table 12 on page 48.

If all the channel walls in contact with Pb-17Li would be covered with a 10 μm thick insulation layer consisting mainly of pure aluminum, this would result in a total Al mass in the whole blanket of 360 kg. The Al blended with the steel contained in the first wall and in the breeding region would correspond to an extra Al concentration in MANET of 175 wppm and 300 wppm, respectively, i.e., less than the original Al impurity of 500 wppm. The contribution of the 500 wppm of Al in MANET to the total specific activity in MANET results from activation calculations described in [5] and amounts to only 0.005 at shutdown (mainly from Al-28) and falls off sharply to the order of 10^{-10} after one month. At very long decay times (10^5 years) it comes back to the order of 10^{-3} due to the long-lived Al-26 isotope (Table 12 on page 48, 7th column). A similar behavior is found for the γ -dose rate. Here the contribution of the 500 wppm of Al in MANET amounts to a fraction of 0.015 at shutdown, falls off to the order of 10^{-8} after 1 year and comes back to 0.03 after 10^5 years (Table 12 on page 48, last column). Consequently, the contribution of a 10 μm insulation layer equivalent to an extra Al content of 200-300 wppm is below the 1 % range in terms of specific activity and γ -dose rate. Even a 50 μm thick layer would be uncritical.

A different problem may arise in the Pb-17Li dose rate due to sputtering and corrosion products carried by the liquid metal. This has not been assessed and is to be seen in the context of on-line purification.

3.0 Energy Sources for Mobilization

Energy sources in upset or accidental conditions are seen in (a) plasma disruptions, (b) delayed plasma shutdown after cooling disturbances, (c) decay heat, (d) work potential for pressurised coolants, and (e) exothermic chemical reactions. This section summarises the energy sources for the dual coolant blanket based on the inventories described in 2.0 on page 3. An overview of the energy sources (a) to (e) is given in Table 13 on page 49.

3.1 Energy Liberated during Plasma Disruptions

Plasma disruptions can cause local evaporation of first wall material or mobilization of adhesive dust. This is a common and unresolved problem of first wall protection and dust processing and is not considered here. The energy source is essentially the stored energy in the plasma which is typically of the order of 1 GJ and, hence, is small compared to other energy sources discussed in the following subsections.

3.2 Energy due to Delayed Plasma Shutdown

Delayed plasma shutdown after a sudden cooling disturbance will bring any first wall to melt within seconds. The energy source is simply the time integral of fusion power from the cooling disturbance to complete shutdown. For instance, for the reference plasma shutdown scenario (plasma is shutdown 1 s after cooling disturbance; at that time the internal heat source disappears instantaneously and the first wall surface heat flux decreases linearly down to zero in 20 s) the energy transmitted to the first wall is 4.2 GJ and to the blanket 0.8 GJ per GW of fusion power (ignoring that a large fraction of the 4.2 GJ goes to the divertor). This scales up to 9.2 GJ to the first wall and 1.8 GJ into the blanket for a 2.2 GW reactor.

3.3 Decay Heat

The decay heat is the governing feature in managing the cooling disturbances like loss of coolant accidents (LOCA) and loss of flow accidents (LOFA) (section 4.0 on page 19) and, in particular, loss of site power or loss of heat sink. The decay heat in the entire blanket amounts to 52 MW after shutdown and declines to 11.8 MW after 1 h, 1.53 MW after 1 d, 1.07 MW after 1 month, and 0.48 MW after 1 year [5]. The accumulated decay heat at several times after shutdown is listed in Table 13 on page 49, ranging from 1.2 GJ for the first minute period to 3200 GJ during the first month.

Table 14 on page 50 and Table 15 on page 51 present average afterheat power densities and total afterheat values for Pb-17Li and MANET in different regions of the blanket and for several time steps after shutdown. The values have been evalu-

ated from 3D FISPACT calculations with multiple radial zones [5], weighted by volumes presented in Appendix A on page 73.

Note: The geometrical model used in Appendix A on page 73 is not identical to the geometrical model used in FISPACT and, therefore, the integral after-heat fall short by about 10 % compared to the values reported in [5] and referred to above.

A dilution factor for the afterheat generation in Pb-17Li to account for external circulation has been applied in the bottom half of Table 14 on page 50 in the same way as was done in the activity assessment in 2.3.2.1 on page 8. In lieu of detailed analyses with given 'in-core' and 'ex-core' sequences this dilution assumption is deemed to be more realistic than the results obtained from stationary FISPACT calculations.

Comparing the total afterheat in the structure (Table 15 on page 51) with that in Pb-17Li (Table 14 on page 50) at different decay times it becomes evident that right after shutdown the heat generation in Pb-17Li would dominate (70 % of the total) if no dilution were considered. With dilution the Pb-17Li contributes 38 % to the total afterheat in the blanket. However the situation changes very fast and after one hour the structure is controlling the power generation. Thus, for short term transients a more realistic assessment of afterheat in Pb-17Li is important, whereas for long term decay heat removal the afterheat of the structure prevails.

The decay heat source has to be seen in connection with the thermal inertia of the blanket and related cooling systems. High thermal inertia limits temperature transients and amplitudes in upset or faulted conditions and, thereby, contributes inherently to minimise potential consequences for a primary initiating event and eases plant control. A measure for the thermal inertia (more precisely, of its inverse value) is the adiabatic temperature evolution of the isolated blanket or of parts of the blanket, like the first wall, the breeding zone, or the shield region. These temperature vs. time curves are plotted in Figure 11 on page 64 and it can be seen that the transient for the isolated first wall is very steep, reaching a temperature rise of about 400 K for the first hour. In contrast, the isolated shield warms up very slowly (about 10 K for the first day), and likewise the Pb-17Li alone. For a mixture of the whole blanket structure (first wall, breeding zone plus shield) including the liquid metal the temperature rise amounts to approximately 280 K within the first day.

In general, one can conclude that the adiabatic transients in isolated portions of the blanket are moderate (except in the first wall), leaving sufficient time for afterheat removal measures, including establishing a natural circulation heat transport. Please note that the temperature rise in the first wall can never reach the values quoted because of the thermal coupling with the breeding zone. It may rather approach the curve obtained for the mixture of the whole blanket.

3.4 Work Potential of Helium Coolant

The first wall cooling system contains 6300 kg of helium at 8 MPa and inlet/outlet temperature of 250/350 °C, i.e., a mean temperature of ≈ 300 °C. The work potential relative to ambient conditions for the total helium inventory is 9.1 GJ. A more realistic scenario is the adiabatic expansion of the helium inventory from one outboard cooling subsystem, comprising three primary loops with an inventory of about 2000 kg (see Table 6 on page 44). The corresponding work potential would be 2.9 GJ. Upon release, this helium would pressurise the vacuum vessel (VV) in the event of an in-vessel pipe rupture to 0.45 MPa (assuming a free volume of 5000 m³). This is probably below the expected design pressure and, hence, would not require an extra expansion volume. In case a high pressure resistance of the vacuum vessel could not be achieved, the required expansion volume would be 14000 m³, when assuming 0.2 MPa as absolute end pressure.

The release times for the helium of one of the two independent outboard cooling subsystems (300 m³) in the case of a double-ended pipe break of different cooling pipes in the primary loop were investigated [11]). Analytical computations assuming reversible adiabatic expansion of the pressurised helium yielded draining times of 1.8/2.9/46 s for inner pipe diameters of 760/600/150 mm which belong to the hot leg, ring collector, and feeders, respectively.

To obtain an estimate of the effects of wall friction and heat transfer from the pipe walls to the helium during outflow, a simple RELAP model was established. The simulated pipe lengths were 100/100/30 m for the diameters 760/600/150 mm mentioned above. Computations with this model resulted in somewhat longer draining times of 2.5/4.3/72 s for the respective diameters. The longer release times are due to dissipation of kinetic energy by friction and due to decreasing density of the outflowing gas stream by heat supply from the pipe walls. Figure 12 on page 65 shows the depressurization of one of the two outboard first wall cooling subsystems after a double-ended break in either the hot leg, ring collector, or in one feeder.

The momentum forces of the gas stream immediately at the beginning of the discharge were calculated according to the mass flows and velocities obtained with the RELAP model to 2000/1100/54 kN per side for the pipe diameters of 760/600/150 mm.

The minimum release time for the helium in case of a double-ended break of a cooling channel in the first wall (cross sectional area 25 mm × 25 mm, reversible adiabatic expansion) was estimated to 22 minutes. This long time span is due to the small cross sectional area of a first wall cooling channel, which limits the outstreaming mass flow to some kilograms per second.

It should be noted that there exists a potential for the release of the helium from both cooling subsystems at a time into the vacuum vessel in case of a crack in a segment box extending over adjacent cooling channels, each one pertaining to one cooling subsystem. Then the end pressure and, if necessary, the expansion volume discussed above would be doubled if the failure occurred in an outboard first wall. A similar occurrence in the inboard first wall would have less consequences because of the smaller helium inventory.

3.5 Exothermic Chemical Reactions Review

Chemical reactions may occur between Pb-17Li and water, air, nitrogen if used as inert gas in rooms, and concrete in various accident scenarios. These processes have been reviewed in [12] and found to be moderate. A summary of the experimental evidence from a literature review is given below.

3.5.1 Pb-17Li-Water Reactions

In contrast to pure lithium the reaction of Pb-17Li with water in an open pool has been found to be modest or mild in a wide range of melt temperature (up to 600 °C) [13], [14]. Water addition to excess alloy melt at 600 °C led to an increase in the temperature to 652 °C. The amount of hydrogen released during the reaction was $0.22 \text{ molH}_2/\text{molH}_2\text{O}$.

Small scale reaction kinetics studies have shown low reactivity of Pb-17Li with water, compared with other alloys with higher lithium concentration or with pure lithium [15]. For instance, the reaction rate of lithium with steam was found to be two orders of magnitude higher than that of Pb-17Li at 400 °C. Measured mean reaction rates were $0.05 \text{ mol}/(\text{m}^2\text{s})$ and $4.0 \text{ mol}/(\text{m}^2\text{s})$ for Pb-17Li and Li, respectively.

On the other hand, an intermediate scale Pb-17Li alloy-steam reaction test [16] identified areas of concern to be pressurization of containment and generation of hydrogen, aerosols, moderately high temperatures and corrosive reaction products. In this test, steam at 335 °C was injected into 200 kg of Pb-17Li at 500 °C at a rate of 5 g/s for 325 s. Practically all of the lithium in the alloy reacted to form Li_2O and LiOH. The amount of hydrogen generated was $0.56 \text{ molH}_2/\text{molH}_2\text{O}$. The lead in the alloy did not react with steam at this temperatures. The bulk Pb-17Li temperature rose to 870 °C. Aerosols produced from steam reactions of lithium amounted to 0.25 mg per kg alloy. The maximum suspended mass concentration of lead and lithium was 3.9 and $8.4 \text{ mg}/\text{m}^3$, respectively.

At Westinghouse, 500 g of water were injected into 200 kg of alloy at 532 °C [17]. One mole of hydrogen was formed for each mole of water reacted, and aerosols were released.

Cooperative experiments were conducted by the European Union and the U.S. Department of Energy at the Joint Research Centre in Ispra. In these tests, 1.2 kg of

water were injected into 475 kg of lithium-lead alloy at 500 °C [18]. 99.8 % of the water reacted and 0.57 mol of hydrogen was released per mol of water reacted. The water injection was self limiting. The maximum pressure attained in the reaction module was limited to that of the water supply pressure. Aerosol products identified were mainly lead and lead oxide.

Simulation of water leakages into liquid alloy with the BLAnket Safety Test facility (BLAST) in Ispra has shown that mixing is the governing factor in the Pb-17Li-water interaction process [15] [19]. It was found that the pressurization in the reaction vessel depends strongly on the hydraulic constraints of the Pb-17Li pool. With a low flow resistance between the reaction vessel and the expansion vessel the pressurization in the reaction vessel did not exceed the water injection pressure. However, with a large flow resistance, pressure pulses in excess of the injection pressure were observed [19]. With view to the vapour explosion hazard it has been concluded in [19] that the BLAST experiments indicated that the chemical reaction is self-limiting and, due to the hydrogen generation and production of solid LiOH and Li_2O , the melt is partially isolated from the water so that energetic vapour explosions appear unlikely under the mixing conditions tested. Reservations have been made to this statement for small leakage.

3.5.2 Pb-17Li-Air Reactions

The reaction of an eutectic lithium-lead pool with air (humidity less than 70 %) is negligible. Even at 900 °C no violent reaction could be observed [20].

Low reaction rates (weight gain) at temperatures up to 500 °C have also been reported in [21] to range between 0.5 (mg/cm^2)/h at 300 °C and $< 100(mg/cm^2)/h$ at 500 °C in "room air" and 1-2 orders of magnitude less in dry air. Unlike the oxidation of molten lead which is diffusion-controlled, the mechanism of oxidation of molten Pb-17Li has been found to be complex.

Fusion safety tests with Pb-17Li alloy breeder material have been conducted by Westinghouse Hanford Company in cooperation with CEC in Ispra: Tests in air with up to 200 kg of Pb-17Li and spill temperatures of 714 °C show no temperature increase [17]. At 450 °C no aerosol formation and no containment pressurization was observed, only a thin oxide layer was formed on the surface. At 700 °C, some lithium aerosols and lead aerosols were released.

Similarly, JRC-Ispra tests have confirmed that no ignition occurred in 700 - 800 g of Pb-17Li tests up to 1050 °C [20]. But, in heating the alloy to 1050 °C in an open crucible, oxide layers were formed and removed during heat-up.

An alloy spray in air reaction test (HEDL) indicated that there was no significant containment pressurization or temperature increase due to chemical reactions. Pb-17Li at 720 °C was sprayed into air producing lithium and lead aerosols [17].

According to Piet et al. [22], the low severity of the Pb-17Li-air reaction comes from (a) the lower amount of lithium in Pb-17Li (0.68 % by mass), (b) the ability of the lead to act as heat sink and (c) lithium becoming depleted near the Pb-17Li surface. Furthermore, the chemical activity of lithium is relatively low even in the liquid alloy [23].

3.5.3 Pb-17Li-Nitrogen Reactions

A lithium-lead alloy pool reaction test with nitrogen showed that nitrogen is the least reactive of atmosphere gases. The alloy-nitrogen reaction up to 500 °C produced no aerosols, very little heat and no combustible gas [23].

3.5.4 Pb-17Li-Concrete Reactions

A medium scale Pb-17Li-concrete reaction test was performed at HEDL [17]. 200 kg of lithium-lead alloy at 600 °C were poured on top of a basalt concrete test article. The reaction was quite mild. In fact, heaters had to be turned on to keep the test at 600 °C. Hydrogen gas was released, about $0.45 \text{ molH}_2/\text{molLi}$, close to the maximum of $0.5 \text{ molH}_2/\text{molLi}$. Thus, the Pb-17Li did react with water of the concrete. However, there was no reaction with solid concrete constituents.

4.0 Fault Tolerance

The following analyses of electromagnetic forces induced by disruptions, temperature transients caused in the case of loss-of-coolant accidents (LOCA), and temperature distribution during handling have been performed in order to show, whether this blanket system is tolerant against transients and accidental conditions.

4.1 Behavior during Electromagnetic Transients

Electromagnetic forces and induced stresses caused by disruptions have been analysed with the CARIDDI code. The 3D eddy current code has been improved in several aspects, so that it is possible now to take into account toroidally conducting structures and to model a dynamic plasma behavior. Additionally, an interface to the finite element structural program ABAQUS has been developed.

With the latest version of CARIDDI which is now running on UNIX workstations further computations for the dual coolant blanket concept were conducted. For example, the loading of the blanket subjected to a so-called design plasma disruption (20 MA decaying linearly within 20 ms) was determined. The maximum von-Mises stress of 73 MPa occurs in the internal radial wall next to the side wall (see Figure 13 on page 66). Because of the assumed rigid fixing at the back side the eddy current damping of the structural parts is small (Figure 14 on page 67) and may be neglected.

With the aid of the new features of CARIDDI and with a simple model for the blanket the influence of the electrically conducting first wall was investigated. In contrary to earlier investigations the time function of the plasma current was not prescribed any more. Instead, the plasma current could evolve freely. Nevertheless, the results proved the former expectation that a toroidally conducting first wall will reduce the induced currents and forces. Although the magnetic induction increases decisively in the domain of the blanket, the currents and forces will be reduced by a factor of 3 to 5. This is caused by the increased time constant of the resistive-inductive system built by the plasma, first wall, and the blanket. This increased time constant is linked to smaller time gradients of the magnetic induction.

An important effect neglected up to now is the large toroidal current (some MAs) which together with the magnetic field of the poloidal field coils will produce extra forces. They will try to bend the first wall around the toroidal axis. Further computations are needed in this area.

4.2 LOCA Temperature Transients

Temperature transients have been studied for instantaneous loss-of-coolant scenarios with leaks in one of the three primary coolant subsystems attached to one blanket segment (2 helium subsystems for the first wall and one Pb-17Li subsystem for the breeding zone), and in the NaK circuit.

4.2.1 LOCA in one First Wall Helium Subsystem

The analysis has been performed with the FIDAP code for a reference loss-of-coolant accident scenario as already defined in 3.2 on page 13. Since the cooling of the first wall is done in multiple passes, a representative 3D model containing a half-channel of both cooling systems was generated for each pass. The helium inlet temperature of a pass is determined by the outlet temperature of the preceding pass. It was assumed that there is no heat exchange between the first wall and the breeding zone. The calculations were carried out with the average value for the surface heat flux of 0.4 MW/m^2 to determine the transient helium temperature. For the calculations of the temperature distribution in the structure, carried out in a second step with a finer 2D mesh, the peak value for the surface heat flux of 0.5 MW/m^2 was used. The value of the internal heat sources depends on the poloidal and radial position and is taken from neutronics calculations.

The maximum steady state temperatures obtained in the first wall are $515 \text{ }^\circ\text{C}$ in the equatorial midplane and $521 \text{ }^\circ\text{C}$ at the blanket top. This is in good agreement with the calculations carried out with ABAQUS. The maximum transient temperatures, reached about 13 s after LOCA occurrence, were obtained at the edge of a blanket segment, where the hotter coolant channels belonged to the cooling system that failed. They are $615 \text{ }^\circ\text{C}$ in the equatorial midplane and $620 \text{ }^\circ\text{C}$ at the blanket top (Figure 15 on page 68). This temperature increase from $521 \text{ }^\circ\text{C}$ (in steady state) to $620 \text{ }^\circ\text{C}$ (transient peak) causes a reduction of the allowable primary stress according to the ASME code from 234 to 166 MPa which is still larger than the actual primary stresses caused by the coolant pressure. Therefore, a failure of the structure is not expected. However, a thermal stress analysis with computed transient temperature distributions has still to be carried out. A more detailed description of the results and the calculational method is given in [24].

4.2.2 LOCA in the Pb-17Li Circuit

A LOCA in the Pb-17Li circuit can cause (a) loss of liquid metal flow in the blanket in case of an ex-vessel leak or (b) a drainage of the Pb-17Li from a blanket segment in case of a major in-vessel leak. For (a) the decay heat in the structure plus Pb-17Li per outboard segment would be 0.77 MW (2.8 % of the normal power), leading to a hypothetical adiabatic temperature increase of 0.4 K/s in the Pb-17Li in the front channel row next to the first wall. This temperature would stabilise at $T_{\text{Pb-17Li}} < T_{\text{He}} + 160 \text{ }^\circ\text{C}$ if the first wall cooling remained intact (T_{He} = helium coolant temperature) and ignoring in a conservative way the heat dissipated to the rear part of the blanket segment. For case (b) with all Pb-17Li removed but

with the first wall cooling systems operating an estimation revealed a maximum structure temperature $T_{structure} < T_{He} + 100\text{ }^{\circ}\text{C}$. At $T_{He} = 350\text{ }^{\circ}\text{C}$ this is slightly above the normal operating temperature. These transients do not threaten the integrity of the structure.

4.2.3 LOCA in the NaK Circuit

A LOCA in the NaK circuit for tritium removal with the consequence of substituting the NaK in the steam generator tube gaps by the cover gas, e.g., argon, would impede the heat transfer coefficient in the steam generator by 1 to 2 orders of magnitude, leading to a strong temperature increase of Pb-17Li at the steam generator outlet. This transient arrives with a delay of $\approx 30\text{ s}$ at the blanket inlet and after further 75 s at the blanket outlet. Therefore, in order to avoid excessive temperatures in the blanket the plasma has to be shutdown within approximately 60 s after drainage of the NaK. The afterheat of less than 3 % of the normal power generation can then be dissipated by the failed steam generator in combination with the first wall cooling circuits. The scenario does not present a safety concern, but the temperature transients need further attention with regard to design limits.

4.3 Temperature Distribution during Handling

The question arose whether active cooling of a blanket segment during handling will be necessary or whether the afterheat could be dissipated via the segment surfaces to the ambient medium. The afterheat generation in the structural material MAN-ET and in the breeder material Pb-17Li decreases by about one and two orders of magnitude within one day after shutdown, respectively (Table 15 on page 51 and Table 14 on page 50). Thus the blanket is assumed to be cooled for at least a period of one day after shutdown before the replacement of a segment can start. Prior to handling it is planned to drain the segment and fill it with gas. In this analysis air or helium are considered as both filling gas and ambient medium.

4.3.1 Temperature Distribution in Gas-filled Segments

The steady-state temperature distribution in the passively cooled blanket segment during handling is defined by the internal heat sources, the heat transport inside the blanket, and the heat emission from the outer surfaces to the environment. For computing the two-dimensional radial-toroidal temperature distribution a simplified geometric model of an outboard blanket segment was established. This blanket model was subdivided into different volume elements reflecting the actual structure from Figure 2 on page 55. Each volume element exchanges energy with the adjacent heat structures and, if it is a structure at the boundary, with the environment. For each of the different volume elements an energy balance was carried out. The energy balances serve as formulae for computing the temperatures in the structures after a short time increment starting from a given initial temperature distribution. For conducting the computations a FORTRAN 77 program was prepared.

The following cases were investigated with the peak temperatures obtained:

Case	Ambient and blanket filling medium	Consideration of heat transport in the gas-filled cooling channels	Peak temperatures ($^{\circ}\text{C}$), when heat emission to the environment	
			from front, rear and side walls	from front and rear wall only
Case I	Air	Yes	215	
Case II	Air	No	222	
Case III	Air	Yes		290
Case IV	Air	No		300
Case V	Helium	Yes	180	
Case VI	Helium	No	188	
Case VII	Helium	Yes		240
Case VIII	Helium	No		255

Figure 16 on page 69 shows radial temperature profiles in the structural material MANET in a radial-poloidal sectional view in the middle of the blanket segment at steady-state conditions for cases I to IV (air as filling and ambient medium). The highest temperatures appear about 20 cm behind the first wall. Under consideration of the heat transport in the air-filled cooling channels they are approximately 215 $^{\circ}\text{C}$ in the case of heat emission from front, rear and side walls (case I) and 290 $^{\circ}\text{C}$ in the case of heat emission from front and rear wall only (case III).

The corresponding curves for helium as filling and ambient medium (cases V to VIII) are shown in Figure 17 on page 70. For cases V and VII the peak temperatures are approximately 180 $^{\circ}\text{C}$ and 240 $^{\circ}\text{C}$. The considerable lower temperatures for helium compared with air are due to the higher thermal conductivity of helium ($\lambda_{\text{he}} \approx 0.144 \text{ W/mK}$, $\lambda_{\text{air}} \approx 0.025 \text{ W/mK}$, $\lambda_{\text{he}}/\lambda_{\text{air}} = 5.8$). This results in a higher heat transfer coefficient for natural convection at the blanket walls. Its value is about $6 \text{ W/m}^2\text{K}$ for air as ambient medium and about $9 \text{ W/m}^2\text{K}$ for helium as ambient medium.

The curves show that the neglect of the heat transport in the gas-filled cooling channels (cases VI and VIII) leads only to a minor elevation of the temperature level. The following table shows the approximate fractions of the different heat transport mechanisms inside the blanket relative to the total heat transport for air and helium:

Contribution of heat transfer mechanism	with Air	with Helium
Conduction in MANET	90 %	88 %
Natural convection and heat conduction in the gap	6 %	8 %
Radiation across the gap	4 %	4 %

The small fraction of the radiation across the gap of only 4 % is due to the low prevailing temperatures in the blanket. This fraction will increase with increasing temperatures. The small fraction of the natural convection and heat conduction in the gap is due to the small magnitude of the apparent thermal conductivity in the

gap which is approximately 0.2 W/mK for air and 0.3 W/mK for helium. This is roughly a factor 100 smaller than the thermal conductivity of MANET which is about 25 W/mK.

Figure 18 on page 71 shows the toroidal temperature profiles in the case of heat emission from front, rear, and side walls obtained with air and helium under consideration of the heat transport in the gas-filled cooling channels for mesh points $n=2$ (first channel row from first wall) and $n=4$ (second channel row). The maximum temperature difference between the center of the segment and the side walls appears at $n=4$. It amounts to 57 °C and 53 °C for air and helium, respectively.

4.3.2 Temperature Distribution in Pb-17Li-filled Segments

The steady-state temperature distribution in the blanket segment during handling with Pb-17Li inside was computed with the finite element code FIDAP. The calculations were based on the following conditions:

- Heat emission to the environment due to natural convection and radiation
- Heat emission from front and back wall (not from side walls)
- Ambient medium air at 1 bar, 25 °C
- Cooling channels in the first wall filled with air at ambient conditions during handling.
- Heat transport inside the blanket due to heat conduction in the structural material and in the liquid metal.

Computations were conducted using (a) the values of the specific afterheat in the structure and in the Pb-17Li at midplane of the outboard blanket, and (b) the poloidal average values. The specific afterheat in Pb-17Li at midplane one day after shutdown was determined to about 520 W/m³. This value is the volume-weighted mean of the specific afterheat in the different radial zones of the outboard blanket segment according to [5]. Taking credit of the dilution factor of 3.5 for the afterheat generation in Pb-17Li due to external circulation during operation, as discussed in 3.3 on page 13, would reduce the afterheat to approximately 150 W/m³. This value was chosen in the analysis. (It is only 2-3 % of the corresponding value in the structure of the breeding zone.)

The result of the computation with maximum internal heat sources at midplane and the mesh grid is illustrated in Figure 19 on page 72. The maximum temperature in the structure amounts to 293 °C. The same computation with air replacing the liquid metal yielded a peak temperature of 349 °C. The corresponding maximum temperatures obtained with the poloidal average values of the specific afterheat are 250 °C with Pb-17Li and 300 °C with air. Thus, due to the small specific afterheat of the liquid metal one day after shutdown and due to its high thermal conductivity, the presence of Pb-17Li in the blanket tends to spread the heat over the blanket and, therefore, lowers the peak temperature inside the blanket.

In conclusion the analysis of the two-dimensional temperature distribution in a dual coolant outboard blanket segment during handling showed that the heat transfer at the outside of the blanket segment due to natural convection and radiation, and the heat transport inside the blanket mainly due to heat conduction in the structure are good enough to prevent hot spots in the structural material which could endanger the integrity of the blanket segment. If the segment is filled with Pb-17Li instead of gas the peak temperatures are even smaller despite the afterheat generation in the liquid metal. Since the computed temperatures are below the temperatures at operating conditions, even in the worst case of totally hampered heat emission from the side walls, it can be concluded that active cooling during handling is not an unconditional requirement, if an ambient heat sink at a temperature level of about 25 °C is available.

5.0 Tritium and Activation Products Release

5.1 Release during Normal Operation

In normal operation the total release of tritium and activation products to the environment should not exceed 1 TBq/d as a guide line. The release is expected to be dominated by the liquid tritium effluents arising from the cooling loops via permeation in the steam generators into the secondary water/steam cycle. For these discharges an upper limit of 20 Ci/d (0.74 TBq/d) is assumed to be achievable (see 2.3.1 on page 7). This leaves little margin for other effluents, for instance originating from primary coolant leakages (into the containment and from there via the plant air detritiation system to the environment) and from other fuel cycle equipment. Those have not been assessed here but conservative estimates performed in the frame of the safety and environmental assessment of fusion power (SEAFP) [25] indicate that they may also range up to close to 1 TBq/d, so that the total releases would exceed the 1 TBq/d guideline. Further assessment is needed in this area.

5.2 Tritium Release in Accidental Situations

For a first judgement on the radiological hazard potential, an assessment has been made on the early dose and chronic dose to the most exposed individual at a distance of 1 km from the point of release caused by the tritium inventory escaping into the vacuum vessel (VV) or containment in the case of a LOCA, and from there to the environment. In this chapter the tritium release from the various fluids and the radiological consequences are discussed.

The accidental tritium release into the vacuum vessel or into the containment in the case of a LOCA is summarised in Table 16 on page 52 along with the radiological consequences to the most exposed individual. The scenario starts from the total tritium inventory in the various fluids (Pb-17Li, helium, and NaK as intermediate fluid in steam generators) from which a certain fraction can escape into the vacuum vessel or some other compartment of the containment upon a LOCA. The envisaged escape fractions are assumed to be a proportion of the escaping fluids and are as follows:

For the breeder material one half of one outboard Pb-17Li subsystem (15 % of the total inventory) is assumed to drain into the vacuum vessel by gravity. The other half will remain in the blanket segments not affected, in the piping and components located below the ring headers (which connect the main circuits with the individual blanket segments at some elevated level, see Figure 5 on page 58). If the LOCA occurred ex-vessel the escape fraction would probably be even smaller than 15 %. These assumptions do not take any credit from isolation valves which would likely reduce the escape fraction to a few percent. For the primary first wall helium

LOCA the whole inventory from one subsystem would escape either into the vacuum vessel or into another compartment. The largest subsystem (for the outboard) comprises 31 % of the total helium inventory (Table 6 on page 44). The NaK system for tritium removal is divided into 10 subsystems (one subsystem per steam generator) with one of the outboard subsystems containing about 12 % of the total NaK. This can be released into the containment but not into the VV.

For the mechanisms that follow the fluid escape into the vacuum vessel or containment, i.e., tritium mobilization (predominantly in elemental form), oxidation, transportation within the containment, and finally release to the environment, it is assumed in a conservative way that no retention occurs in either of these mechanisms. In that case all the tritium contained in the escaped fluid is released to the environment in form of HTO (the more dose effective form compared to HT). To compute the early dose (ED, that is, 7 days exposure plus 50 years integration, no ingestion) from the tritium source term a conversion factor of 0.26 mSv/g-T, and for the chronic dose (EDE, that is, 50 years exposure plus 50 years integration, with ingestion) a factor of 1.6 mSv/g-T has been used [26]. These factors vary with release scenarios by about 3 orders of magnitude as investigated in [27] and the chosen values range close to the upper bound (of 1 mSv/g-T for the early dose and 4 mSv/g-T for the chronic dose).

Thus, the predicted early dose and the chronic dose, respectively, to the most exposed individual resulting from tritium release range from very low values for a NaK spill (0.01 and 0.07 mSv), and still low values for primary helium blowdown (0.5 and 3.1 mSv) to considerable values for Pb-17Li spills (2.2 and 13.7 mSv) when applying this conservative scenario (Table 16 on page 52). The tolerable dose limits, on the other hand, are still under discussion and the spectrum of national regulations is rather wide. Recent recommendations discussed in ITER for various classes of event sequences range from 0.1 mSv/a for likely sequences ($f > 10^{-2}/a$) over 5 mSv/event for unlikely sequences ($10^{-2}/a > f > 10^{-4}/a$) to 5-50 mSv/event for extremely unlikely sequences ($10^{-4}/a > f > 10^{-6}/a$), where f is the rate of occurrence. In SEAFP a value of 100 mSv/event is suggested as a yardstick with the understanding that doses of this level trigger the consideration of evacuation but do not yet mandate it.

Hence, depending on the classification of the events regarded in Table 16 on page 52 and on the established dose limits the early and chronic doses obtained for the tritium releases for in-vessel and ex-vessel LOCAs will probably comply with the dose limits. If a conflict should arise a less conservative assessment would have to be undertaken that could bring down the doses by at least two orders of magnitude, for instance in the areas of mobilization, chemical form of the liberated tritium, and confinement retention (for the latter compare the example in 5.3 on page 27).

5.3 Activation Products Release in the case of a Pb-17Li LOCA

As an example for the potential activation products release from the liquid metal breeder to the environment and its radiological consequences to the public a major spill of Pb-17Li into the vacuum vessel is discussed in terms of activation products inventory, liberation of liquid metal (LM) into the vacuum vessel, mobilization of radionuclides from the spill, retention by the containment, release to the environment, and the radiological impact to the most exposed individual. The assessment is made on a nuclide-by-nuclide basis revealing the Hg-203 isotope as the major contributor to the early dose.

The underlying scenario for the in-vessel LOCA in a Pb-17Li subsystem (similar to the one discussed in 5.2 on page 25) is as follows:

- The plant has operated for 20000 hours at full power, radioactive nuclides generated are taken from FISPACT calculations for the outboard front channels at midplane, which are assumed to be diluted by radial and poloidal averaging and by circulation in loops (dilution factor f_D)
- Major break in the Pb-17Li confining wall of the outboard segment
- Drainage of one half of one Pb-17Li subsystem's inventory into the vacuum vessel (2.1×10^6 kg), postulating that isolation valves fail to close
- Collection of spilled Pb-17Li mass at the bottom of vacuum vessel without break of vacuum (non-oxidising atmosphere) rendering a spill height of 2 m, a spill surface of 200 m², and a mixed mean temperature of 350 °C
- Evaporation of radionuclides into VV at low pressure (vacuum) for a time period of 7 days after which the melt is assumed to be solidified, no condensation within the VV.
- Break of vacuum in the VV and release of 100 % of evaporated nuclides into the second containment (instantaneously)
- Release of fraction, f_R , of the nuclides from the containment into the atmosphere within 1 hour (usual release scenario), where f_R = containment retention factor
- Dispersion of released source term and 7 day early exposure to the most exposed individual at 1 km distance (without ingestion).

Then the 7 day early dose, ED, is computed by equation 2.

$$ED = M \sum_i \hat{a}_i f_{D_i} f_{M_i} f_{R_i} d_i \quad (2)$$

where

\hat{a}_i	peak specific activity of nuclide i in 1 kg of Pb-17Li irradiated in out-board front channels at midplane (stationary) after 20000 h,
f_{D_i}	dilution factor for peak specific activity due to radial and poloidal averaging and due to circulation in loops for nuclide i ,
f_{M_i}	evaporation fraction of nuclide i (mobilization factor) from spilled Pb-17Li with free surface of 200 m^2 during given time period,
f_{R_i}	containment retention factor as a result of plate-out at cold walls and/or vent/filter system for nuclide i ,
M	spill mass of Pb-17Li at bottom of VV,
d_i	specific early dose of radionuclide i per unit source term (1×10^9 Becquerel) released at the containment boundary.

Table 17 on page 52 lists all these factors for the twelve leading nuclides out of 73 nuclides that have been traced, and their contribution to the early dose to the most exposed individual. The following comments refer to the choice of parameters in addition to the definitions given to equation 2:

The specific activity for the nuclides (except for tritium in HTO form) is taken from activation analyses [4]. The activity for HTO of 1.41×10^9 Bq/kg-LM corresponds to the tritium inventory of 57 g in 15×10^6 kg of Pb-17Li (Table 7 on page 44).

The dilution factor accounting for the radial and poloidal averaging of the specific activity and for circulation in external loops has generally been assumed to be 1/30 (with 1/3.5 for circulation multiplied by 1/8.6 for spatial averaging). This assumption seems appropriate for long-lived isotopes resulting from simple reactions in the neutron and gamma field, like Hg-203, Zn-65, Cd-113m, Cd-113, Ag-110m. The Po-210 build-up does not follow this simple rule and an approximate dilution factor of 0.11 has been deduced from investigations performed by Fischer et al. [28]. The same factor has arbitrarily been assumed for Bi-210 (although in this case of no importance). Finally, the tritium activity in Pb-17Li is not diluted in the circuit, since it is determined by the extraction process to 57 g in 15×10^6 kg of Pb-17Li.

Evaporation fractions (mobilization data) from a Pb-17Li spill are reported in [29] for a number of elements, like Po, Bi, Pb, Tl, Hg, and Li. They have been adapted for a spill temperature of 350 °C and a free surface of 200 m^2 in vacuum for the elements mentioned. For the other elements, where no such data are available, mobilization data collected in the SEAFP study [25] are adopted which, however, include already the containment retention factor (see below).

The containment retention factor was generally set to 0.01, presuming that 99 % of the airborne nuclides will condense at containment walls and/or will be retained in the containment air detritiation system. For those elements where only combined

mobilization fractions, including the retention, are available, the containment retention factor was set to 1.

The specific early dose per unit source term released to the environment was used from dose calculations performed by Raskob [26], [27]. They hold for a seven day exposure in 1 km distance without ingestion, release height of 10 m, a release duration of 1 h.

The result of this conservative LOCA scenario for a spill of one half of the Pb-17Li inventory contained in one subsystem shows that the total early dose resulting from 73 nuclides amounts to 11 mSv (Table 17 on page 52). This is a moderate value when compared to the dose limits already discussed in 5.2 on page 25. It must be noted that 98.9 % of the early dose arises from a single nuclide, Hg-203, due to the extremely high vapour pressure of mercury, leading to a complete release of Hg-203 from the spill. This will be a matter of further investigation [29]. The contribution of Po-210 and tritium to the early dose are only 0.7 % and 0.2 %, respectively. (Note that in this scenario the containment retention factor for HTO was set to 0.01 instead of 1 as used in 5.2 on page 25.)

6.0 Waste Generation and Management

Only the commissioning waste (no operational waste) is considered here. The masses, volumes, radioactivities, and afterheat are summarised in Table 18 on page 52. The total amount of radioactivity in the blanket structure (MANET) sums up to 7.5×10^7 TBq at shutdown for all inboard and outboard segments according to 2.3.2 on page 8, one half of which being in the small volume of the first wall and only $\approx 5\%$ being in the large volume of the removable shield. The contribution of each radionuclide has been calculated as described in [5] for different cooling times. The dominating nuclides in the activation parameters vary with time and activation parameter. For example, Fe-55 and Mn-54 dominate the specific activity at a cooling time of 1 year, and Nb-91, Ni-63, Nb-93 dominate after 100 years. The contact γ -dose rate per kg of MANET in the first wall ranges up to 1.1×10^5 Sv/h, declining slowly. The IAEA low level waste (LLW) limit of 2×10^{-3} Sv/h is reached after about 10^5 years, and the hands-on limit of 2.5×10^{-5} Sv/h is met not sooner than 3×10^5 years.

The total amount of radioactivity in Pb-17Li is 1.3×10^8 TBq at shutdown, decaying by seven orders of magnitude within 100 years. (The numbers quoted in Table 18 on page 52 for Pb-17Li have been derived from radially and poloidally averaged values for the different blanket parts and account for a dilution factor due to external circulation of 3.5 for the outboard and 4.7 for the inboard.) The following nuclides dominate the specific activity by more than 65 % at various times: Pb-207 (after 0 s), Pb-203 and Pb-204 (after 1 h), Pb-203 (after 1 d), Hg-203 (after 1 month), Tl-204 (after 1 year), Pb-205 and Ag-108 (after 100 years). The contact γ -dose rate of Pb-17Li reaches the LLW limit without any purification after 300 years, the hands-on limit after a few 1000 years. In view of the high lithium enrichment needed (90 atom-% Li-6) the liquid metal breeder is envisaged to be used for several blanket life times or even for more than one reactor life time, since the burnt amount of lithium can be replaced easily.

7.0 Summary and Conclusions

This report summarises the safety considerations for the dual coolant blanket concept, performed essentially in the frame of the European blanket concept selection exercise, in five chapters: (a) blanket materials and toxic materials inventory, (b) energy sources for mobilization, (c) fault tolerance, (d) tritium and activation products release, and (e) waste generation and management. The assessment is based on the latest cooling system design, comprising 10 Pb-17Li circuits and 10 helium circuits for the first wall cooling. The results are summarised below, conclusions with regard to further investigations needed are drawn in 7.2 on page 34.

7.1 Summary of Results

Blanket material and toxic material inventories: The total blanket volume (all in-board and outboard segments, full toroidal coverage) amounts to 1020 m^3 with fractions of 40/41/16/3 percent for steel/Pb-17Li/helium/void, respectively. The loop arrangements account for redundancies, leading to an overpower capacity of 150 % of nominal. Considering this fact, the total Pb-17Li inventory amounts to $14.8 \times 10^6\text{ kg}$ and the total helium inventory amounts to 6300 kg (970 m^3) with 53 - 60 % of the inventory being in the piping.

The tritium inventory in fluids is small, i.e., 57 g in Pb-17Li, $< 6.3\text{ g}$ in helium, and $\approx 0.4\text{ g}$ in NaK. The major part (100 g) is in the cold traps. Activation products inventory in MANET decays slowly, reaching hands-on levels only after very long times (10^5 years). The aluminum contained in the insulation layer contributes to less than 1 %.

Energy sources for mobilization: The main energy sources for mobilization result from decay heat and work potential of helium. The chemical energy potential of lithium contained in the Pb-17Li is also high but the extent of reaction is very limited. The decay heat would cause adiabatic temperature rises in isolated parts of the blanket of about 400 K for the first hour in the first wall, 15 K for the first day in the shield and Pb-17Li, and 270 K for the first day in the mixed material of the outboard blanket. The helium inventory from 1 outboard cooling subsystem would pressurise the vacuum vessel in the case of a LOCA to 0.45 MPa which is below the expected design pressure. The release times are short (few seconds) and the momentum forces of a double-ended major pipe break are high (2000 kN). Chemical reactions between Pb-17Li and water, air, nitrogen, and concrete have been reviewed and found to be moderate.

Fault tolerance: Induced peak stresses caused by disruptions are predicted to be moderate (73 MPa), but the modelling needs refinement. The effect of an electrically conducting first wall was found to reduce the induced currents and forces by a factor of 3 to 5. Short term LOCA temperature excursions in the blanket

structure of the order of 100 K above steady state levels for the assumed cases do not endanger the blanket integrity. Active cooling during handling of a blanket segment is not required if the free convective surrounding gas (air or helium) can be kept at a low temperature level.

Tritium and activation product release: The early and chronic dose for overly conservative tritium release scenarios from Pb-17Li, helium, and NaK are close to, or beyond, dose limits presently discussed. An activation products release scenario from a major Pb-17Li spill yields a moderate early dose of 10 mSv. Hg-203 is by far the dominating nuclide contributing with 98.9 % followed by Po-210 and tritium.

Waste generation: The total amount of structural material from one complete set of blanket segments (without demountable and permanent shield) to be disposed of amounts to 1400 tons (180 m^3) with decay heats one year after shutdown ranging from $1.6 \times 10^4\text{ W/m}^3$ for first wall material down to $1.1 \times 10^3\text{ W/m}^3$ for the breeding zone. In the removable shield the corresponding value is $2.6 \times 10^2\text{ W/m}^3$.

7.2 Conclusions

No insurmountable safety problems have been identified for the dual coolant blanket. Overall, the safety and environmental impact has been judged to be of almost the same level as the one evaluated for the other three European DEMO blanket concepts [30]. Nevertheless, a number of concerns need further investigations or optimization in the five areas addressed:

Blanket material and toxic material inventories: The large Pb-17Li inventory of $15 \times 10^6\text{ kg}$ poses some safety concerns in case of a major LOCA with subsequent potential activation products release to the environment. Improvements can be obtained by (a) reducing the inventory by optimising the liquid metal circuitry (availability versus redundancy, increased flow velocity in piping), (b) appropriate plant layout (isolation valves, steam generator position), (c) improved mobilization modelling (especially Hg evaporation from a Pb-17Li spill).

The tritium inventories in fluids are small and do not raise severe safety concerns to the public in accidental situations. On the other hand, the routine release via steam generators (SG) relies on permeation barriers at the water side of both the helium/water SGs and the Pb-17Li/NaK/water SGs. The reliability and durability of such barriers have still to be proved. Tritium permeation through Pb-17Li pipe walls has not been elucidated but needs attention. Likewise the tritium control in the first wall helium coolant (which is based on the same concept as foreseen for the solid breeder blanket) implies large uncertainties with regard to the amount of tritium permeating from the plasma through the first wall into the helium.

Energy sources for mobilization: The main energy sources for mobilization result from afterheat in the blanket and from work potential of helium coolant. Except for the first few seconds the afterheat is dominated by the decay in the structural material rather than in the Pb-17Li. In the medium and long term (hours and days) the afterheat is moderate compared to the thermal inertia of the system and can be rejected by one of the three separate cooling systems connected to each segment. It is expected, but needs to be proved, that this is also true in the case of natural convection circulation.

The work potential of the helium coolant is moderate compared to purely helium cooled concepts. Yet, an extra expansion volume for the case of a major LOCA seems to be necessary.

The chemical energy potential of lithium is high but the reaction kinetics of Pb-17Li with other media are limited as numerous experiments with water, air, nitrogen, and concrete indicate. A major safety concern is seen in the NaK/water reaction in the SG with potential failure propagation which requires medium scale experiments.

Fault tolerance: Stresses induced by disruptions do not seem to create severe safety concerns at the present state of knowledge. However, large uncertainties still exist in the model with regard to physics phenomena, mechanical boundary conditions, design features, effect of poloidal field coils, and material strength. Further R&D is needed which is not specific to a particular blanket concept.

Short term temperature transients for the LOCA cases investigated are moderate, but the scenarios are to be extended to LOCAs, occurring simultaneously in more than one cooling subsystem, and to loss-of-flow accidents (LOFA). The latter imply also transition periods to achieve natural circulation heat transfer. In those cases more realistic afterheat assessment in Pb-17Li is needed which accounts for the short term decay and for dilution of activation products due to circulation in external circuits. Further attention should also be given to a LOCA in the NaK circuit.

Tritium and activation products release: Some of the release issues have already been addressed in the above paragraph 'blanket material and toxic material inventories'. The release scenarios have to be refined aiming at reducing overly conservative assumptions. In general, this complex is not considered critical for design basis accidents. In particular, the release of Po-210 is no longer regarded as a feasibility issue, since both the generation and the mobilization of this isotope have been overestimated by orders of magnitude in former investigations.

Beyond design basis accidents have not been considered according to the terms of reference. Likewise, the issues related to the first wall material (chemical reactions,

tritium liberation, dust) have been deliberately ignored in the blanket concept selection exercise, because they are in common to all blanket concepts.

Waste generation: The amount of high level waste is dominated by the structural material MANET, the choice of which was a common working hypothesis in the blanket concept selection exercise. Developing a low activation material is a world-wide effort. Pb-17Li should be recycled leaving minor waste problems.

Acknowledgement

The authors gratefully acknowledge the collaboration of H. Tsige-Tamirat and U. Fischer from the "Institute für Neutronenphysik und Reaktortechnik" in providing numerous data files from their 3D FISPACT analysis in addition to the references cited from which the information on nuclide concentration, activities, and afterheat contained in this report has been extracted.

8.0 References

- [1] M. Dalle Donne et al.: European DEMO BOT solid breeder blanket - Status Report to be published.
- [2] S. Malang, M. Tillack, et al.: Development of self-cooled liquid metal breeder blankets, FZKA 5581, September 1995.
- [3] K. Kleefeldt, F. Dammel, K. Gabel: Safety and environmental impact of the BOT helium cooled solid breeder blanket for DEMO, FZKA 5754, 1996.
- [4] H. Tsige-Tamirat, FZK internal note, June 1994.
- [5] H. Tsige-Tamirat, U. Fischer: Three-dimensional activation and afterheat analyses for the dual coolant breeder blanket, FZKA 5675.
- [6] P. Norajitra: FZK internal report, January 1993.
- [7] S. Malang, K. Schleisiek et. al.: Dual coolant blanket concept, KfK5424, November 1994.
- [8] S. Malang et al.: DEMO-relevant Test Blankets for NET/ITER, Part 1: Self-cooled Liquid Metal Breeder Blanket, KfK 4908, (1991).
- [9] J. Wagner et al.: SEAFP internal report, February 1994.
- [10] M. A. Fütterer, X. Raepsaet, E. Proust: Tritium permeation through helium-heated steam generators of ceramic breeder blankets for DEMO, Proc. ISFNT-3, Los Angeles, Ca., June 27 - July 1, 1994, Part C 225-232.
- [11] K. Gabel, FZK internal report (July 1995).
- [12] K. Kleefeldt et al., FZK internal report (Aug. 1993)
- [13] D. W. Jeppson, L. D. Muhlestein, R. F. Keough, S. Cohen: Fusion Reactor Blanket Material Safety-Compatibility Studies, HEDL-SA-2747, AIChE Fall 1982 Annual Meeting, Los Angeles, November 1982.
- [14] G. Kuhlbörsch, H. Dietz, D. Droste: The Chemical Behavior of Eutectic Lithium-Lead Alloy $Li_{17}Pb_{83}$ in Comparison with Pure Lithium, Commission of the European Community, JRC, Ispra, (October 1983).
- [15] H. Kottowski, O. Kranert, C. Savatteri, C. Wu, M. Corradini: Studies with Respect to the Estimation of Liquid Metal Blanket Safety, Fus. Eng. Des. 14 (1991) 445-458.
- [16] D. W. Jeppson, L. D. Muhlestein: Safety considerations of lithium alloy as a fusion reactor breeding material, Fus. Tech. 8 (1985), 1385-1391.
- [17] M. Corradini, D. W. Jeppson: Lithium Alloy Chemical Reactivity with Reactor Materials: Current State of Knowledge, Fus. Eng. Des. 14 (1991) 273-288.
- [18] D. W. Jeppson, C. Savatteri: Consequences of Water Injection into High-Temperature $Li_{17}Pb_{83}$ Alloy Breeder Material, Fusion Technology Vol. 19, May 1991, 1403-1408.
- [19] C. Savatteri, A. Gemelli: Lithium-lead/water interaction. Large break experiments, ISFNT-2, Karlsruhe, FRG, June 2-6, Fusion Eng. Des. 17 (1991) 343-349.

- [20] G. Kuhlbörsch, F. Reiter: Physical properties and chemical reaction behavior of $Li_{17}Pb_{83}$ related to its use of a fusion reactor blanket material, Nucl. Eng. Des./Fus. 1 (1984), 195-203.
- [21] H. Feuerstein et al.: Oxidation of Pb-17Li in air between 25 and 650 °C - Comparison with lead, KfK 4927 (1992).
- [22] S. J. Piet, D. W. Jeppson, L. D. Muhlestein, M. S. Kazimi, M. L. Corradini: Liquid Metal Chemical Reaction Safety in Fusion Facilities, Fusion Eng. Des. 5, (1987), 273-298.
- [23] H. U. Borgstedt: Chemische Eigenschaften des flüssigen Blanketstoffs Pb-17Li, KfK 4620, 1989.
- [24] F. Dammel, FZK internal report, 1994.
- [25] J. Raeder, I. Cook, F. H. Morgenstern, E. Salpietro, R. Bünde, E. Ebert: Safety and environmental assessment of fusion power (SEAFP), Report of the SEAFP Project, EURFUBRU XII-217/95, June 1995.
- [26] W. Raskob: private communication, June 1995.
- [27] W. Raskob: Dose assessment for releases of tritium and activation products into the atmosphere performed in the frame of two fusion related studies: ITER-EDA and SEAFP, Fusion Technology 1994, Proceedings of the 18th SOFT, Karlsruhe, Germany, 22-26 August 1994, 1473-1476.
- [28] U. Fischer, E. Wiegner: Production of Po210 in Pb-17Li: Assessment of Methodological and Data Related Uncertainties, Proc. 17th Symp. on Fus. Tech., Rome, Italy 14-18 Sept. 1992, 1719-1723.
- [29] H. Feuerstein, FZK internal report, Mai 1995.
- [30] K. Kleefeldt, G. Marbach, T. Porfiri: EU DEMO blanket concepts safety assessment - Final report of Working Group 6a of blanket concept selection exercise, FZK report to be published.
- [31] Speakeasy Computing Corporation, 224 south Michigan ave., Chicago, Illinois 60604, USA.

9.0 Tables

Table 1. Thermal power and redundancy factors for primary cooling circuits					
Blanket Region and Coolant	Thermal power per segment (MW)	No. of blanket segments	No. of primary circuits	Redundancy factor	Power capacity per circuit or total (MW) (nominal power in brackets)
Outboard blanket (Pb-17Li)	23.1	48	2 × 3	1.5	277 (185)
Inboard blanket (Pb-17Li)	13.8	32	1 × 4	1.33	147 (110)
Total blanket (Pb-17Li) (48 Outboard + 32 Inboard Segments)	1550	80	10		2250 (1550)
Outboard blanket (helium)	6.9	48	2 × 3	1.5	83 (55)
Inboard blanket (helium)	5.8	32	2 × 2	2	93 (46)
Total blanket (helium) (48 Outboard + 32 Inboard Segments)	517	80	10		870 (517)
Total blanket (Pb-17Li + helium)	2067	80	20		3120 (2067)

Table 2. Geometrical data of blanket Pb-17Li circuit components (outboard)						
Pipe section or component	Number parallel branches	Pipe Dia. [m]	Pipe Length [m]	Pipe Area [m ²]	Total Volume [m ³]	Total Mass [kg]
1 out of 6 Pb-17Li circuits (1 m/s, nominal power 185 MW)						
- 1 hot leg	1	1.15	40	1.04	41.5	391000
- 1 cold leg to pump	1	1.14	10	1.03	10.3	97700
- 1 cold leg from pump	1	1.14	10	1.03	10.3	97700
- 1 inlet ring collector	1	.93	16	.68	10.9	104000
- 1 outlet ring collector	1	.94	16	.69	11.1	104000
8 outboard segment circuits						
- 8 inlet feeders	8	.33	12	.085	8.2	78200
- 8 outlet feeders	8	.33	12	.087	8.3	78200
Subtotal primary Pb-17Li piping			284		100.6	951000
Other primary circuit components						
blanket segments	8	-	-	-	54.6	517000
steam generator (Pb-17Li side)	1	-	-	-	22.5	213000
pump	1	-	-	-	3	28600
purification system	1	-	-	-	1	9530
expansion vessel (cold leg)	1	-	-	-	4	38100
expansion vessel (degaser)	1	-	-	-	4	38100
Total for 1 primary Pb-17Li circuit			284		189.7	1795000
Total for 6 primary Pb-17Li circuits			1704		1138	10.77E6

Table 3. Geometrical data of blanket Pb-17Li circuit components (inboard)						
Pipe section or component	Number parallel branches	Pipe Dia. [m]	Pipe Length [m]	Pipe Area [m ²]	Total Volume [m ³]	Total Mass [kg]
1 out of 4 Pb-17Li circuits (1 m/s, nominal power 110 MW)						
- 1 hot leg	1	.83	40	.55	21.9	206000
- 1 cold leg to pump	1	.83	10	.54	5.41	51500
- 1 cold leg from pump	1	.83	10	.54	5.41	51500
- 1 inlet ring collector	1	.72	25	.41	10.2	96800
- 1 outlet ring collector	1	.72	25	.41	10.3	96800
8 inboard segment circuits						
- 8 inlet feeders	8	.25	15	.051	6.1	58100
- 8 outlet feeders	8	.25	15	.051	6.2	58100
Subtotal primary Pb-17Li piping			350		65.4	619000
Other primary circuit components						
blanket segments	8	-	-	-	23.04	218000
steam generator (Pb-17Li side)	1	-	-	-	11.3	107000
pump	1	-	-	-	1.5	14300
purification system	1	-	-	-	1	9530
expansion vessel (cold leg)	1	-	-	-	3	28600
expansion vessel (degasser)	1	-	-	-	3	28600
Total for 1 primary Pb-17Li circuit			350		108.2	1025000
Total for 4 primary Pb-17Li circuits			1400		433	4100000

Table 4. Geometrical data of first wall helium circuit components (outboard)						
Pipe section or component	Number parallel branches	Pipe Dia. [m]	Pipe Length [m]	Pipe Area [m ²]	Total Volume [m ³]	Total Mass [kg]
1 out of 6 helium circuits (60 m/s, nominal power 55 MW)						
- 1 hot leg	1	.76	40	.45	18.0	106
- 1 cold leg to pump	1	.69	10	.38	3.8	26.5
- 1 cold leg from pump	1	.68	10	.37	3.7	26.5
- 1 inlet ring collector (120 deg.)	1	.56	40	.24	10.0	70.7
- 1 outlet ring collector (120 deg.)	1	.62	40	.30	12.0	70.7
16 outboard segment circuits						
- 16 inlet feeders	16	.14	16	.015	3.9	28.3
- 16 outlet feeders	16	.15	16	.019	4.8	28.3
Subtotal primary helium piping			652		56	357
Other primary circuit components						
blanket segments	16/2	-	-	-	23	148
steam generator (helium side)	1	-	-	-	9.4	60.6
circulator	1	-	-	-	1	7.2
clean-up system	1	-	-	-	10	72
Total for 1 primary helium circuit			652		99.4	645
Total for 6 primary helium circuits			3912		596	3868

Table 5. Geometrical data of first wall helium circuit components (inboard)

Pipe section or component	Number parallel branches	Pipe Dia. [m]	Pipe Length [m]	Pipe Area [m ²]	Total Volume [m ³]	Total Mass [kg]
1 out of 4 helium circuits (60 m/s, nominal power 46 MW)						
- 1 hot leg	1	.80	40	.50	20.0	118.3
- 1 cold leg to pump	1	.73	10	.42	4.2	29.6
- 1 cold leg from pump	1	.72	10	.41	4.1	29.6
- 1 inlet ring collector (180 deg.)	1	.51	60	.20	12.3	88.7
- 1 outlet ring collector (180 deg.)	1	.56	60	.25	15.0	88.7
16 inboard segment circuits						
- 16 inlet feeders	16	.13	20	.013	4.1	29.6
- 16 outlet feeders	16	.14	20	.016	5.0	29.6
Subtotal primary helium piping			820		64.7	414
Other primary circuit components						
blanket segments	16/2	-	-	-	7	45.2
steam generator (helium side)	1	-	-	-	10.5	67.8
circulator	1	-	-	-	1	7.2
clean-up system	1	-	-	-	10	72
Total for 1 primary helium circuit			820		93.2	606.2
Total for 4 primary helium circuits			3280		373	2425

Circuit or System	Pb-17Li		Helium	
	Volume (m ³)	Mass (kg)	Volume (m ³)	Mass (kg)
Outboard cooling circuit	190	1.8 × 10 ⁶	99.4	645
Inboard cooling circuit	108	1.03 × 10 ⁶	93	606
Outboard cooling subsystem (3 circuits)	569	5.49 × 10 ⁶	298	1934
Inboard cooling subsystem (4 circuits for Pb-17Li, 2 circuits for helium)	433	4.1 × 10 ⁶	187	1213
All outboard cooling circuits (% in blanket/piping/components)	1138	10.8 × 10 ⁶ (29/53/18)	596	3868 (23/55/22)
All inboard cooling circuits (% in blanket/piping/components)	433	4.1 × 10 ⁶ (21/60/18)	373	2425 (8/68/24)
Total cooling circuits (not including ancillaries)	1571	14.8 × 10 ⁶	969	6293

Blanket region or system	Total mass inventory (kg)	Tritium (g)
Breeder material (Pb-17Li)	1.5 × 10 ⁶	57
Primary first wall coolant (helium)	6300	< 6.3
Tritium removal fluid (NaK)	41,000	0.38
Steam system	not assessed	< 1.7
Tritium recovery system	mainly in cold traps	≈100
Structural material (total)	3.2 × 10 ⁶	≈4.4
First wall	10 ⁵	2.6
Breeding zone	1.3 × 10 ⁶	1.8
Shield	1.8 × 10 ⁶	0.006

Table 8. Specific and total activity in Pb-17Li. Average values have been evaluated for the whole inboard (center, top, and bottom part) and outboard (center and top part) from FISPACT calculations [5]. The assumed dilution due to circulation is only a first approximation.

Specific and Total Activity in Pb-17Li of Dual Coolant Blanket							
Blanket Region	Decay time					Volume (m ³)	Mass (kg)
	0 s	1 d	1 y	10 y	500 y		
Specific Activity in Breeding Zone from FISPACT calculations (Bq/kg)							
Breeding region total average inboard	3.28E+13	6.87E+11	3.23E+09	3.71E+08	4.80E+06	92	872,000
Breeding region total average outboard	3.26E+13	6.99E+11	2.97E+09	3.82E+08	3.87E+06	328	3,102,000
Total Activities in Breeding Zone from FISPACT calculations (Bq)							
Breeding region total inboard	2.86E+19	5.99E+17	2.82E+15	3.24E+14	4.19E+12		
Breeding region total outboard	1.01E+20	2.17E+18	9.21E+15	1.18E+15	1.20E+13		
Total Breeding Region inboard plus outboard	1.30E+20	2.77E+18	1.20E+16	1.51E+15	1.62E+13		
Specific Activities in Breeding Zone as calculated divided by dilution factor of 3.5 and 4.7, respectively (Bq/kg)							Dilution
Breeding region total average inboard	6.98E+12	1.46E+11	6.87E+08	7.89E+07	1.02E+06		4.70
Breeding region total average outboard	9.31E+12	2.00E+11	8.49E+08	1.09E+08	1.11E+06		3.50
Total Activities in Breeding Zone as calculated divided by dilution factor of 3.5 and 4.7, respectively (Bq)							
Breeding region total inboard	6.09E+18	1.27E+17	5.99E+14	6.88E+13	8.91E+11		
Breeding region total outboard	2.89E+19	6.20E+17	2.63E+15	3.39E+14	3.43E+12		
Total Breeding Region inboard plus outboard	3.50E+19	7.47E+17	3.23E+15	4.07E+14	4.32E+12		

Specific and Total Activity in Structure (MANET) of Dual Coolant Blanket							
Blanket Region	Decay time					Volume (cm ³)	Mass (kg)
	0 s	1 d	1 y	10 y	500 y		
Specific Activities in Midplane (Bq/kg)							
First wall region midplane average inboard	5.79E+14	3.55E+14	2.07E+14	1.82E+13	2.73E+09		
First wall region midplane average outboard	6.56E+14	4.02E+14	2.35E+14	2.06E+13	3.03E+09		
Breeding region midplane average inboard	3.95E+13	1.78E+13	8.63E+12	8.10E+11	4.99E+08		
Breeding region midplane average outboard	4.19E+13	2.49E+13	1.39E+13	1.21E+12	6.42E+08		
Shield region midplane average inboard	2.03E+13	5.76E+12	1.79E+12	2.34E+11	2.72E+08		
Shield region midplane average outboard	4.84E+12	1.41E+12	4.53E+11	5.76E+10	7.08E+07		
Specific poloidally averaged Activities (Bq/kg)							
First wall region total average inboard	2.43E+14	1.48E+14	8.53E+13	3.83E+12	1.35E+09	5,054,000	38,916
First wall region total average outboard	4.46E+14	2.72E+14	1.58E+14	1.39E+13	2.18E+09	7,488,000	57,658
Breeding region total average inboard	1.60E+13	6.50E+12	2.92E+12	1.93E+11	2.34E+08	58,990,000	454,223
Breeding region total average outboard	2.78E+13	1.63E+13	9.02E+12	7.85E+11	4.64E+08	103,000,000	793,100
Shield region total average inboard	8.74E+12	2.43E+12	7.43E+11	9.90E+10	1.17E+08	98,510,000	758,527
Shield region total average outboard	3.48E+12	1.01E+12	3.19E+11	4.06E+10	5.16E+07	132,310,000	1,018,787
Total Activities (Bq)							
First wall region total inboard	9.46E+18	5.74E+18	3.32E+18	1.49E+17	5.25E+13		
First wall region total outboard	2.57E+19	1.57E+19	9.13E+18	8.02E+17	1.26E+14		
Breeding region total inboard	7.29E+18	2.95E+18	1.32E+18	8.76E+16	1.06E+14		
Breeding region total outboard	2.20E+19	1.29E+19	7.15E+18	6.23E+17	3.68E+14		
Shield region total inboard	6.63E+18	1.84E+18	5.64E+17	7.51E+16	8.85E+13		
Shield region total outboard	3.54E+18	1.02E+18	3.25E+17	4.13E+16	5.25E+13		
Total Blanket	7.46E+19	4.02E+19	2.18E+19	1.78E+18	7.94E+14		

Table 9. Specific and total activity in structural material. Average values have been evaluated for the whole inboard (center, top, and bottom part) and outboard (center and top part) from FISPACT calculations [5].

Table 10. Specific and total activity in Pb-17Li after various decay times. This includes dilution factors of 3.5 for the outboard and 4.7 for the inboard due to circulation					
Blanket Region Inboard or Outboard	0 s	1 d	1 y	10 y	500 y
Specific Activity Inboard (Bq/kg)	7.0E12	1.5E11	6.9E08	7.9E07	1.0E06
Specific Activity Outboard (Bq/kg)	9.3E12	2.0E11	8.5E08	1.1E08	1.1E06
Total Activity Inboard (Bq)	2.9E19	6.0E17	2.8E15	3.2E14	4.2E12
Total Activity Outboard (Bq)	1.0E20	2.2E18	9.2E15	1.2E15	1.2E13
Total Activity Inboard plus Outboard (Bq)	1.3E20	2.8E18	1.2E16	1.5E15	1.6E13

Table 11. Total and mixed mean specific activity in different regions of the blanket structure			
Blanket Region Inboard or Outboard	Steel Inventory (10 ³ g/k)	Total Activity after 10 y (Bq)	Mixed mean Specific Activ- ity after 10 y (Bq/kg)
First wall region inboard	39	1.5E17	3.8E12
First wall region outboard	58	8.0E17	1.4E13
Breeding region inboard	454	8.8E16	1.9E11
Breeding region outboard	793	6.2E17	7.9E11
Shield region inboard	759	7.5E16	9.9E10
Shield region outboard	1019	4.1E16	4.1E10
Total inboard and outboard	3121	1.8E18	5.8E11

Table 12. Activation and dose rate of aluminum in MANET. 500 wppm of Al in MANET contribute to less than 1 % to the total activity in MANET. (Data refer to the first wall and are taken from FISPACT calculations [5]).

ACTIVITY AND DOSE RATE OF AL IMPURITIES IN MANET							
Time after shutdown	Time after shutdown (s)	Activity of 0.05 % Al in MANET Bq/kg-MANET)	Dose Rate of 0.05 % of Al in MANET (Sv/h)	Specific Activity in MANET (Bq/kg)	Dose Rate in MANET (Sv/h)	Fraction Al Activity of total Activity	Fraction Al Dose of total Dose
0 s	0.00E+00	2.99E+12	1.66E+03	5.67E+14	1.10E+05	5.27E-03	1.51E-02
10 min	6.00E+02	1.61E+11	7.26E+01	5.33E+14	9.75E+04	3.02E-04	7.45E-04
1 h	3.60E+03	2.00E+09	1.08E+00	4.94E+14	7.93E+04	4.05E-06	1.36E-05
1 d	8.64E+04	8.63E+08	4.78E-01	3.52E+14	1.27E+04	2.45E-06	3.76E-05
1 month	2.59E+06	6.23E+04	4.62E-05	3.10E+14	1.09E+04	2.01E-10	4.24E-09
1 year	3.15E+07	6.23E+04	4.62E-05	2.05E+14	4.66E+03	3.04E-10	9.91E-09
10 years	3.15E+08	6.23E+04	4.62E-05	1.81E+13	4.50E+01	3.44E-09	1.03E-06
100 years	3.15E+09	6.23E+04	4.62E-05	6.28E+09	5.69E-02	9.92E-06	8.12E-04
1200 years	3.78E+10	6.22E+04	4.61E-05	1.78E+09	5.41E-02	3.49E-05	8.52E-04
13200 years	4.16E+11	6.15E+04	4.56E-05	2.89E+08	3.58E-02	2.13E-04	1.27E-03
111300 years	3.51E+12	5.59E+04	4.15E-05	5.62E+07	1.31E-03	9.95E-04	3.17E-02

Table 13. Energy sources for mobilization	
Energy source	Energy (GJ)
Plasma disruptions (localised)	≈1
Delayed plasma shutdown (reference scenario)	11
Decay heat integrated over:	
1 minute	1.2
1 hour	50
1 day	550
1 month	3200
Work potential of helium coolant	9.1
Chemical energy potential	
Li/water reaction	2300
Li/oxygen reaction	3900

Afterheat Power Density and total Afterheat in Pb-17Li of Dual Coolant Blanket							
Blanket Region	Decay time					Volume (cm ³)	Mass (kg)
	0 s	1 h	1 day	1 month	1 year		
Afterheat power density in liquid breeder from FISPACT calculations (W/cm ³)							
Breeding region total average inboard	7.62E-02	2.22E-03	3.91E-04	1.31E-05	2.68E-06	92,000,000	872,000
Breeding region total average outboard	7.70E-02	2.11E-03	4.03E-04	1.19E-05	1.93E-06	328,000,000	3,102,000
Total afterheat in liquid breeder as from FISPACT calculations (W)							
Total breeding region inboard	7.01E+06	2.04E+05	3.60E+04	1.20E+03	2.46E+02		
Total breeding region outboard	2.53E+07	6.93E+05	1.32E+05	3.89E+03	6.32E+02		
Total breeding region inboard plus outboard	3.23E+07	8.97E+05	1.68E+05	5.09E+03	8.78E+02		
Afterheat power density in liquid breeder from FISPACT divided by dilution factor of 3.5 and 4.7, respectively (W/cm ³)							Dilution
Breeding region total average inboard	1.62E-02	4.72E-04	8.33E-05	2.78E-06	5.69E-07		4.70
Breeding region total average outboard	2.20E-02	6.04E-04	1.15E-04	3.39E-06	5.50E-07		3.50
Total afterheat in liquid breeder from FISPACT divided by dilution factor of 3.5 and 4.7, respectively (W)							
Total breeding region inboard	1.49E+06	4.35E+04	7.66E+03	2.56E+02	5.24E+01		
Total breeding region outboard	7.22E+06	1.98E+05	3.78E+04	1.11E+03	1.80E+02		
Total breeding region inboard plus outboard	8.71E+06	2.41E+05	4.54E+04	1.37E+03	2.33E+02		

Table 14. Afterheat power density and total afterheat in Pb-17Li. Average values have been evaluated for the whole inboard (center, top, and bottom part) and outboard (center and top part) from FISPACT calculations [5]. The assumed dilution due to circulation is only a first approximation.

Table 15. Afterheat power density and total afterheat in structural material. Average values have been evaluated for the whole inboard (center, top, and bottom part) and outboard (center and top part) from FISPACT calculations [5].

Afterheat power density and total Afterheat in Structural Material (MANET) of Dual Coolant Blanket							
Blanket Region	Decay time					Volume (cm ³)	Mass (kg)
	0 s	1 h	1 day	1 month	1 year		
Afterheat in midplane (W/cm ³)							
First wall region midplane average inboard	7.43E-01	5.18E-01	6.98E-02	5.85E-02	2.53E-02		
First wall region midplane average outboard	8.44E-01	5.89E-01	7.93E-02	6.65E-02	2.87E-02		
Breeding region midplane average inboard	6.48E-02	4.64E-02	5.21E-03	3.77E-03	1.78E-03		
Breeding region midplane average outboard	5.54E-02	3.87E-02	5.77E-03	4.69E-03	1.98E-03		
Shield region midplane average inboard	4.14E-02	3.05E-02	2.43E-03	1.53E-03	9.35E-04		
Shield region midplane average outboard	9.71E-03	7.14E-03	5.63E-04	3.54E-04	2.17E-04		
Afterheat poloidally averaged (W/cm ³)							
First wall region total average inboard	3.15E-01	2.20E-01	2.98E-02	2.48E-02	1.06E-02	5,054,000	38,916
First wall region total average outboard	5.76E-01	5.76E-02	5.43E-02	4.55E-02	1.96E-02	7,488,000	57,658
Breeding region total average inboard	2.78E-02	2.00E-02	2.05E-03	1.40E-03	6.90E-04	58,990,000	454,223
Breeding region total average outboard	3.69E-02	2.76E-02	3.84E-03	3.09E-03	1.30E-03	103,000,000	793,100
Shield region total average inboard	1.79E-02	1.32E-02	1.04E-03	6.58E-04	4.10E-04	98,510,000	758,527
Shield region total average outboard	6.99E-03	5.14E-03	3.98E-04	2.48E-04	1.51E-04	132,310,000	1,018,787
Total Afterheat (W)							
First wall region total inboard	1.59E+06	1.11E+06	1.51E+05	1.25E+05	5.38E+04		
First wall region total outboard	4.31E+06	4.31E+05	4.07E+05	3.40E+05	1.47E+05		
Breeding region total inboard	1.64E+06	1.18E+06	1.21E+05	8.27E+04	4.07E+04		
Breeding region total outboard	3.80E+06	2.84E+06	3.96E+05	3.18E+05	1.33E+05		
Shield region total inboard	1.76E+06	1.30E+06	1.02E+05	6.48E+04	4.04E+04		
Shield region total outboard	9.25E+05	6.80E+05	5.27E+04	3.28E+04	1.99E+04		
Total Blanket	1.40E+07	7.54E+06	1.23E+06	9.64E+05	4.35E+05		

Table 16. Early and chronic dose for accidental tritium release from fluids. (Estimates for in-vessel and ex-vessel LOCAs without retention)

Type of fluid	Total tritium inventory (g)	Fraction escaping into		Source term (g)	Early dose (mSv)	Chronic dose (mSv)
		Vacuum vessel	Containment			
Breeder Material (Pb-17Li)	57	≈0.15	< 0.15	≈10	2.2	13.7
Primary first wall coolant (helium)	6.3	0.31	0.31	≈2	0.51	3.1
Intermediate tritium removal fluid (NaK)	0.38	0	0.12	0.04	0.012	0.07

Table 17. The twelve largest contributors to the early dose in case of a Pb-17Li spill. (Spill of 2.1×10^6 kg of Pb-17Li rendering 200 m^2 of free surface)

Nuclide	Peak specific activity (Bq/kg-LM)	Dilution factor	Evaporation fraction	Containment retention factor	Specific early dose (Sv/1E9Bq)	Early dose (Sv)
Hg-203	1.43E+11	0.033	1.00E+00	1.00E-02	1.10E-07	1.09E-02
Po-210	1.08E+09	0.11	5.00E-04	1.00E-02	6.44E-05	8.03E-05
HTO	1.41E+09	1	1	0.01	7.03E-10	2.07E-05
Zn-65	3.74E+09	0.033	1.00E-04	1.00E+00	3.38E-07	8.76E-06
Cd-113m	1.96E+08	0.033	1.00E-04	1.00E+00	2.93E-06	3.98E-06
Cd-109	4.02E+08	0.033	1.00E-04	1.00E+00	3.26E-07	9.08E-07
Bi-210	1.26E+09	0.11	1.00E-06	1.00E+00	1.46E-06	4.25E-07
Ag-110m	2.67E+09	0.033	1.00E-06	1.00E+00	1.47E-06	2.72E-07
Tl-202	8.80E+10	0.033	5.00E-06	1.00E-02	1.08E-07	3.29E-08
Co-58	8.24E+08	0.033	1.00E-06	1.00E+00	3.93E-07	2.24E-08
Pb-203	6.82E+12	0.033	1.30E-07	1.00E-02	3.28E-08	2.02E-08
Zn-69m	1.12E+08	0.033	1.00E-04	1.00E+00	2.18E-08	1.69E-08
Total early dose						1.10E-02

Table 18. Radioactive waste of the blanket system. (after 20000 hours of full power operation)

Blanket region or system	Total mass (kg)	Total volume (m^3)	Total radioactivity in Bq after			Decay heat after 1 y (W/m^3)
			1 y	10 y	500 y	
Breeder Material (Pb-17Li)	15×10^6	1600	1.2×10^{16}	1.5×10^{15}	1.6×10^{13}	0.57
Structural material (total)	3.2×10^6	407	2.2×10^{19}	1.8×10^{18}	7.9×10^{14}	see below
First wall	1×10^5	13	1.2×10^{19}	9.4×10^{17}	1.8×10^{14}	1.6×10^4
Breeding zone	1.3×10^6	162	8.5×10^{18}	7.1×10^{17}	4.7×10^{14}	1.1×10^3
Shield	1.8×10^6	231	8.9×10^{17}	1.2×10^{17}	1.4×10^{14}	2.6×10^2
Insulating layers ($10 \mu\text{m}$)	360	0.13	7×10^9	7×10^9	7×10^9	3×10^{-2}

10.0 Figures

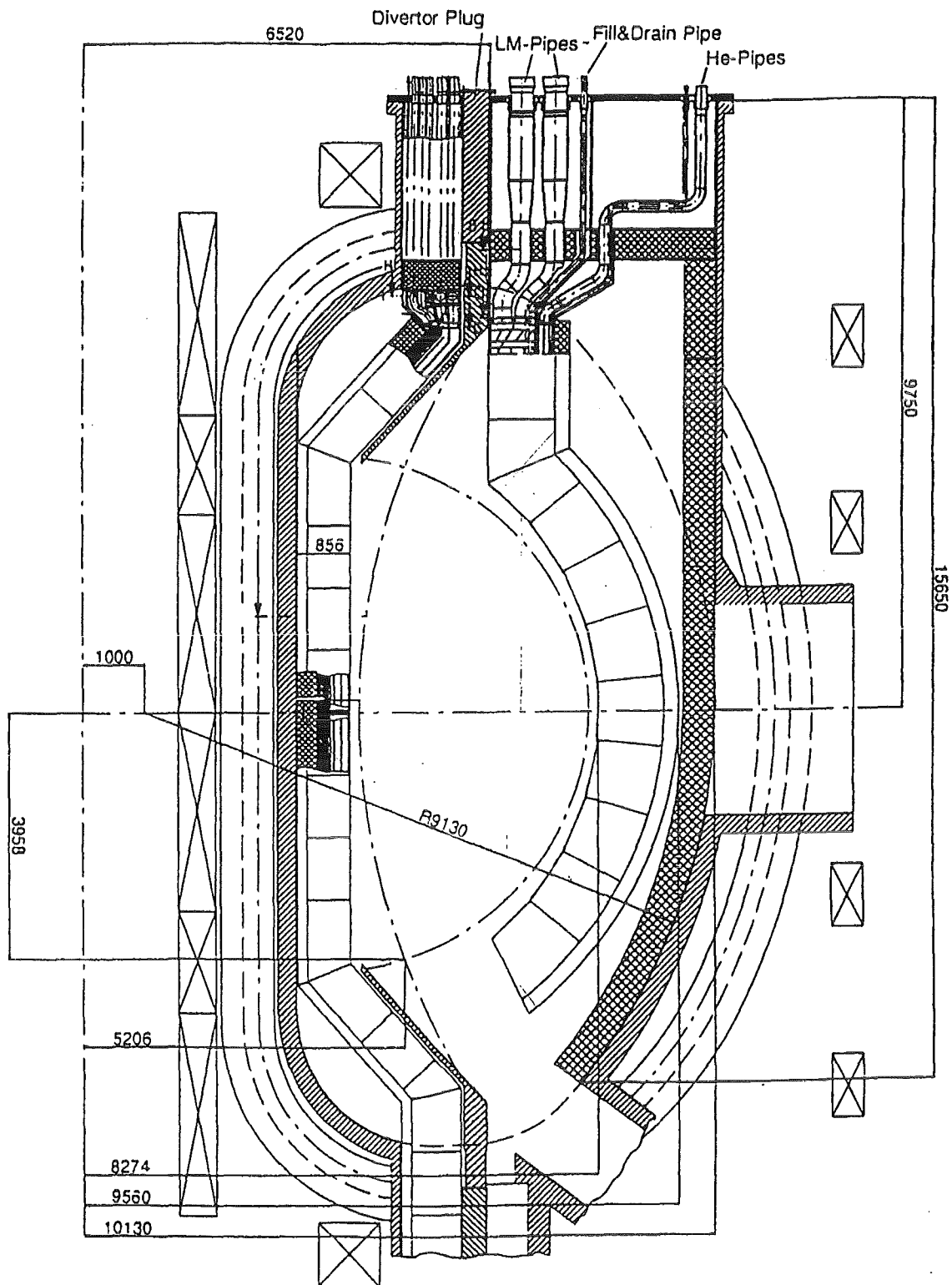
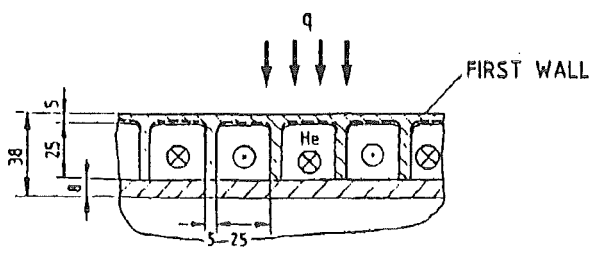
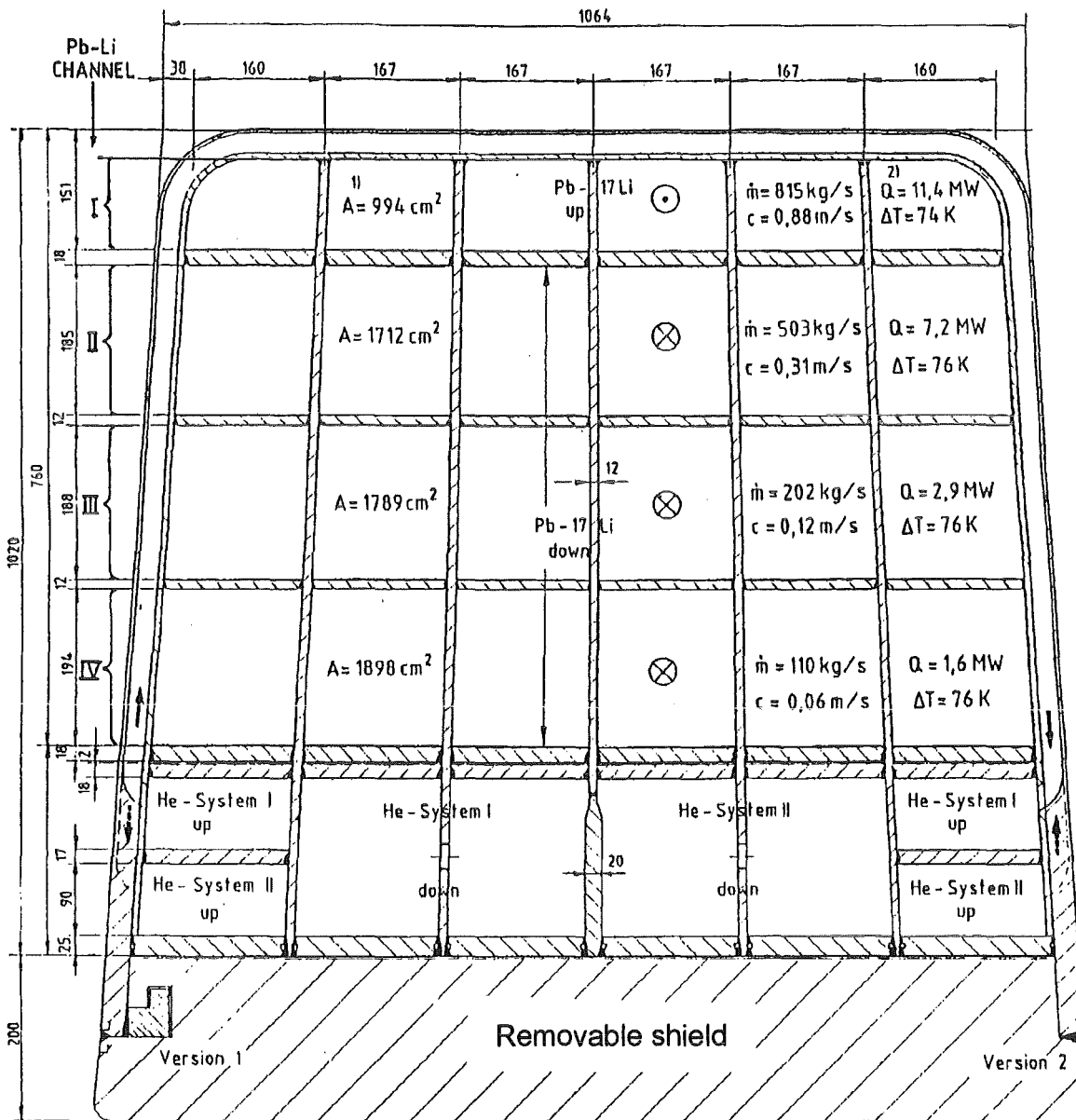


Figure 1. DEMO cross section of the dual coolant blanket. The blanket parts considered include the outboard central and top part, and the inboard central, top, and bottom parts (see text in 2.1 on page 3 and main dimensions in Table 19 on page 73).



M. 15

Figure 2. Cross sectional view of the outboard blanket segment at midplane. Note that the thickness of the removable shield has been increased in the latest design [7] from 200 mm to 246 mm (see 2.1 on page 3).

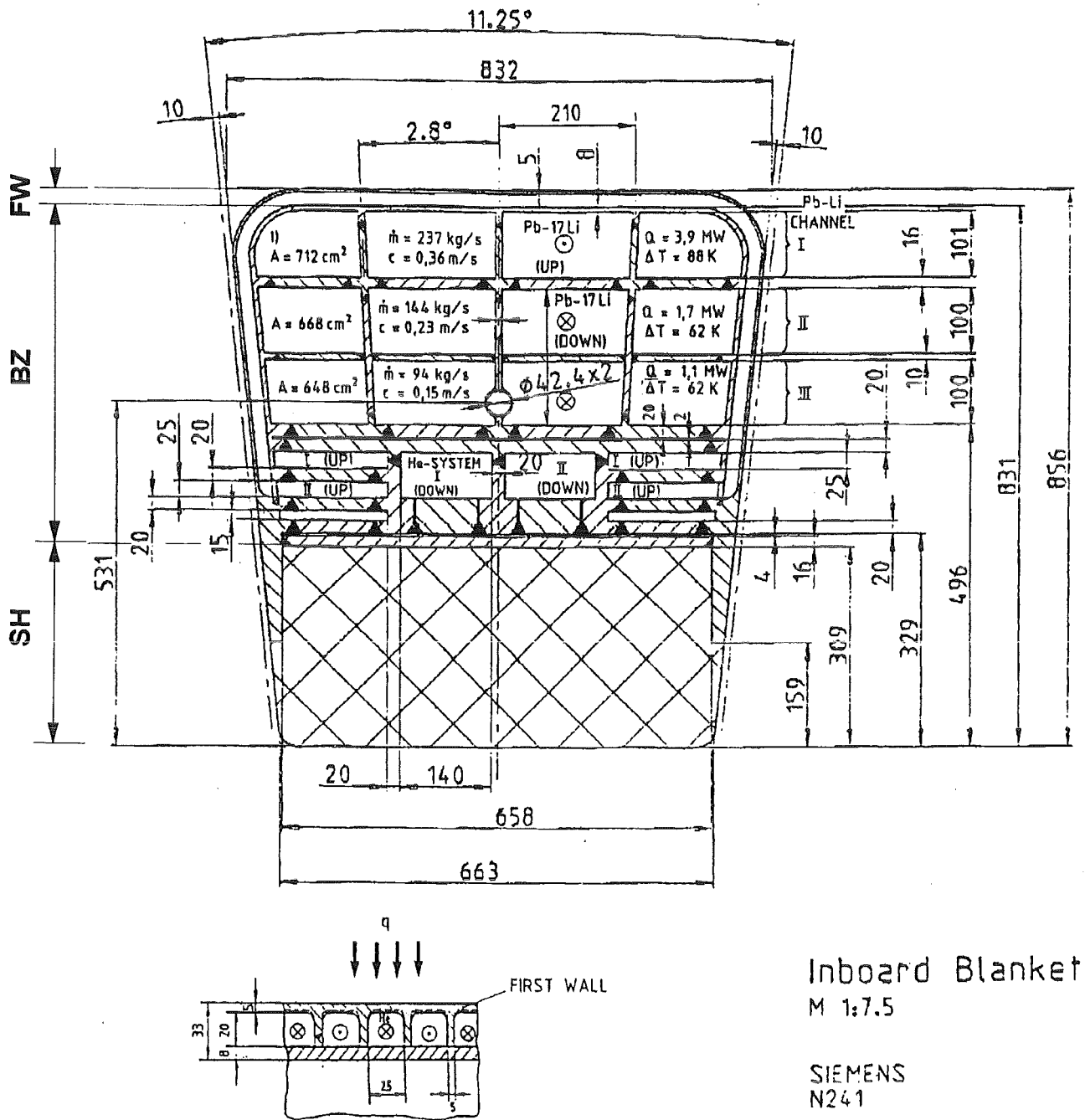


Figure 3. Cross sectional view of the inboard blanket segment at midplane. For discussions of activity three radial zones have been defined, i.e., first wall, breeding zone, and shield with thicknesses of 3.3 cm, 51.4 cm, and 30.9 cm, respectively (see 2.1 on page 3).

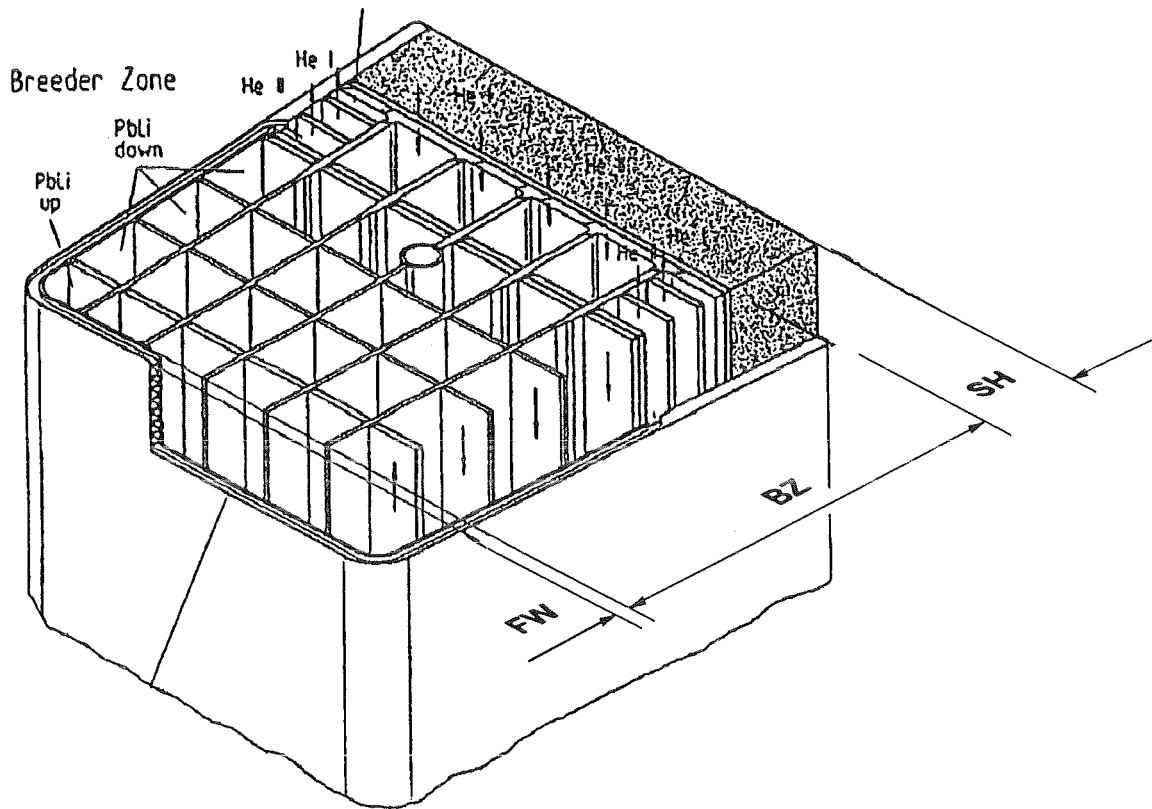


Figure 4. Perspective view of the dual coolant blanket (outboard). For discussions of activity three regions are introduced as indicated, i.e., first wall (FW = 3.8 cm), breeding zone (BZ = 98.2 cm), and shield region (SH = 20 cm), see 2.1 on page 3.

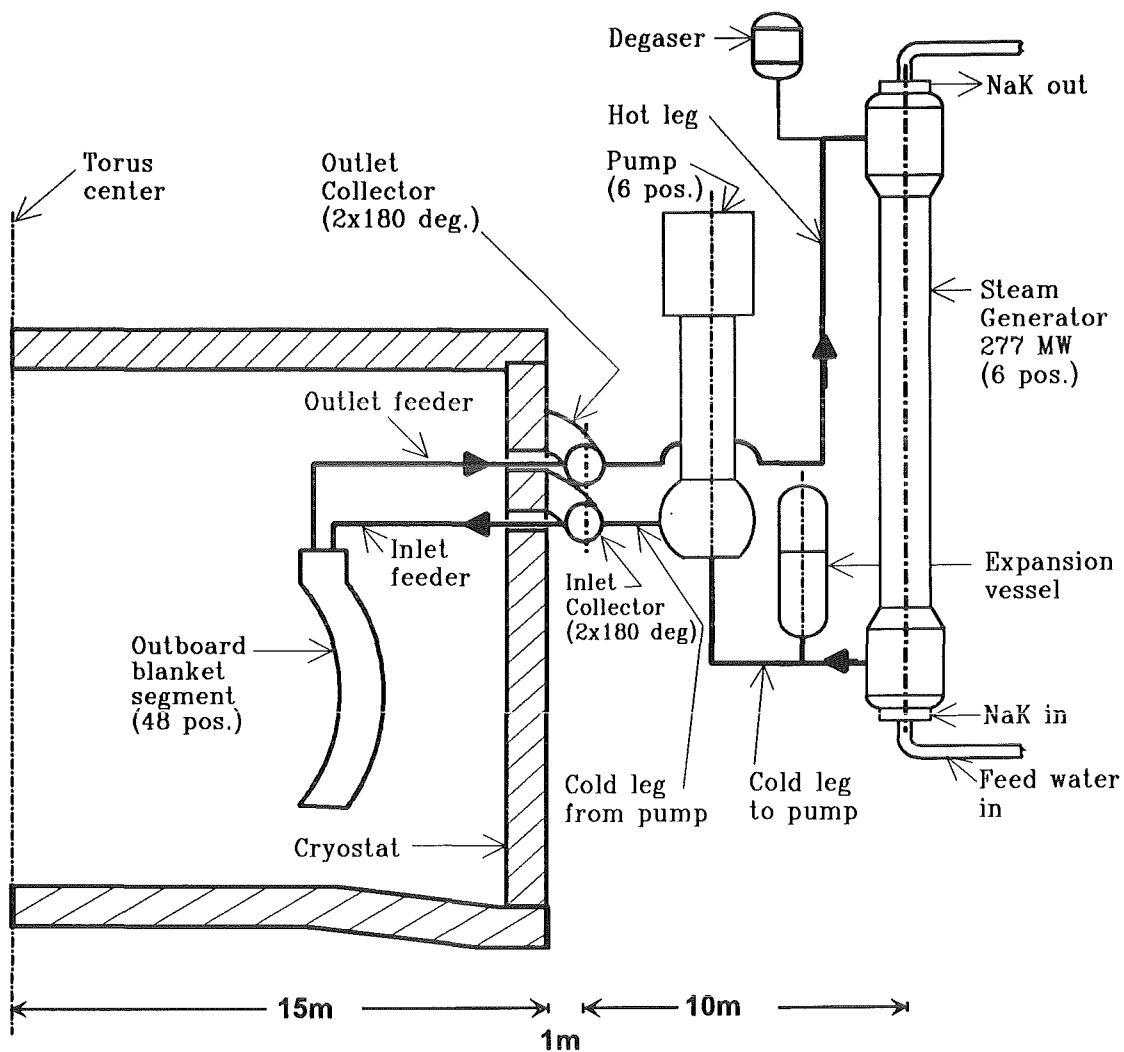


Figure 5. Schematic diagram of a Pb-17Li cooling circuit for the outboard blanket. Shown are the main circuit components and pipe sections of 1 out of 6 primary loops. Three such loops are connected via common inlet and outlet collectors to form a subsystem to provide redundancy in case of a failure in one of the main circuits outside of the collectors (see description in 2.2.1 on page 4).

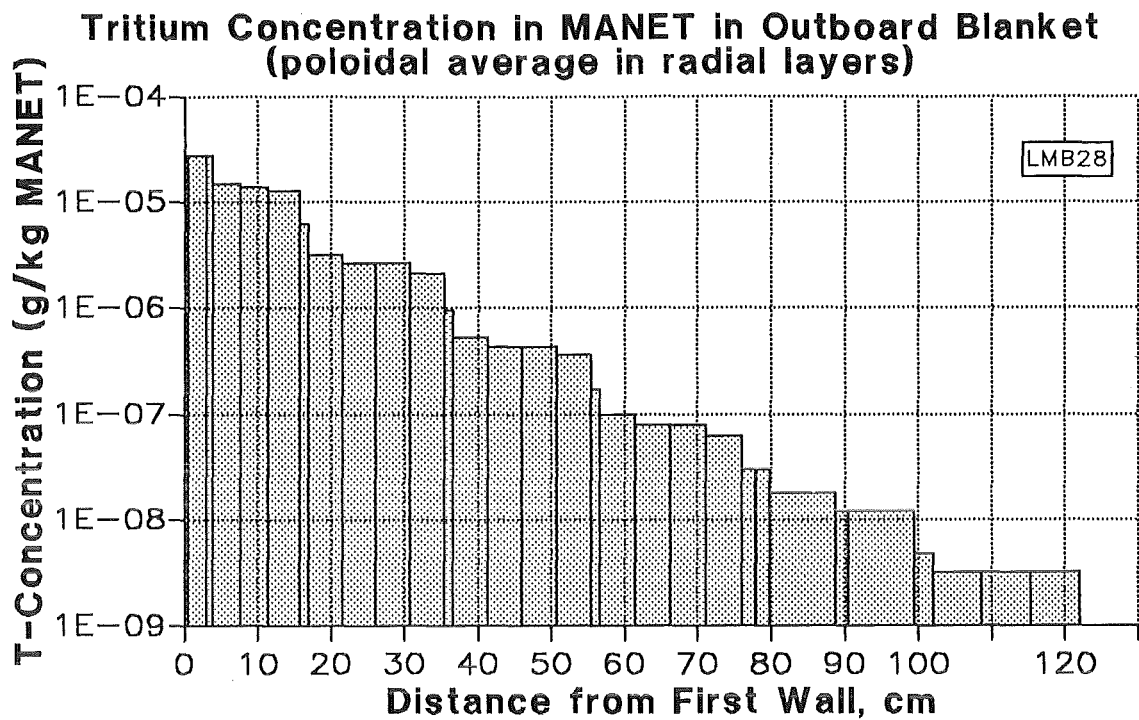


Figure 6. Tritium concentration in MANET in the outboard blanket. Poloidal average in radial layers, reproduced from data in [5], see description in 2.3.1 on page 7.

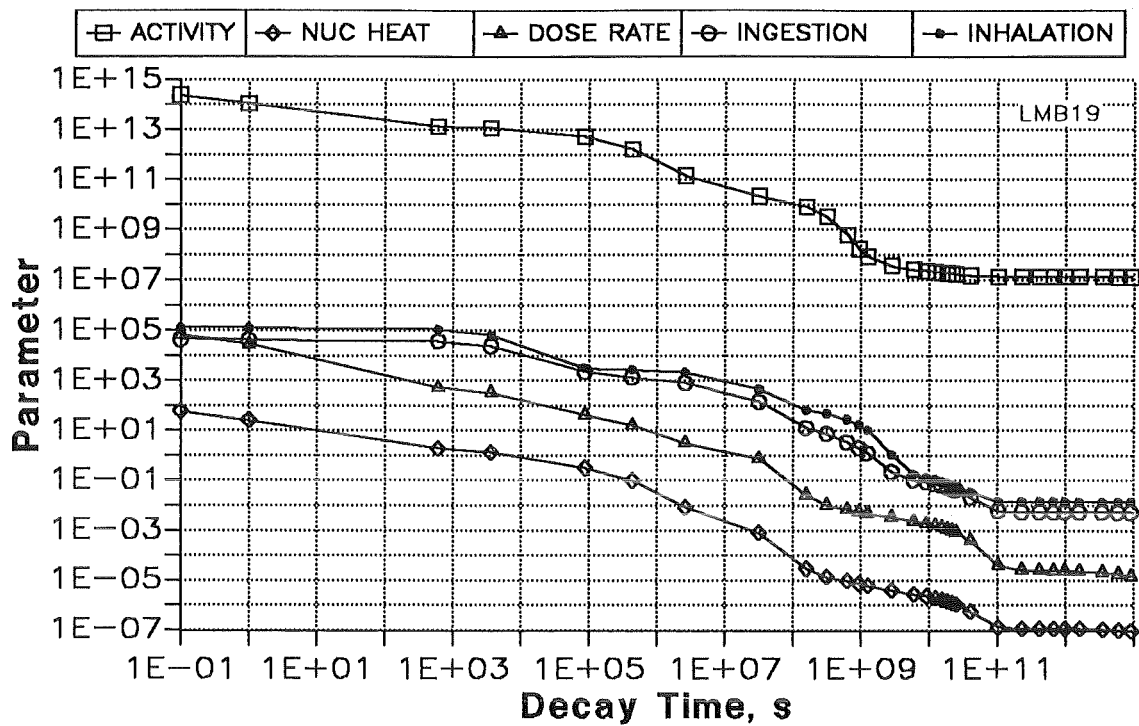


Figure 7. Activation parameters of Pb-17Li of the dual coolant blanket. The parameters have been calculated with FISPACT for the first channel row of the outboard after 20,000 h of operation and refer to 1 kg of Pb-17Li (activity in Bq, nuclear heat in W, γ -dose rate in Sv/h, ingestion in Sv, inhalation in Sv, see 2.3.2.1 on page 8).

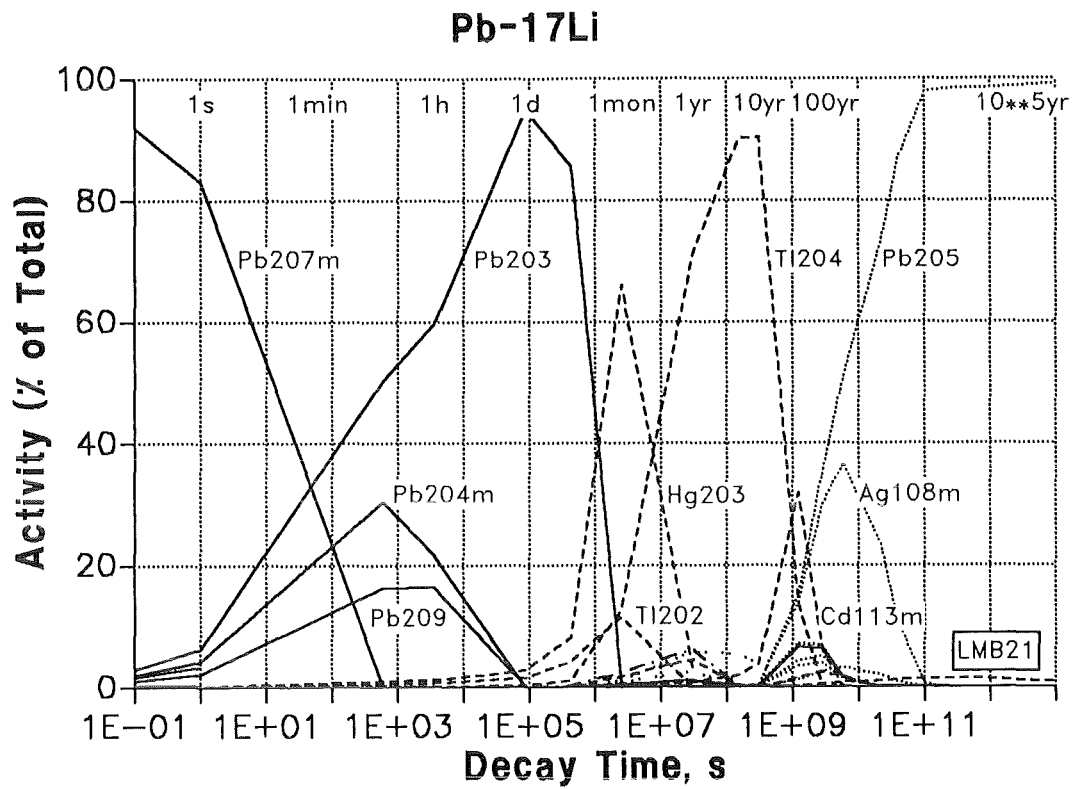


Figure 8. Activity dominating nuclides in Pb-17Li vs. decay time. Plot generated from files provided by Tsige-Tamirat [4] for the outboard blanket front channels (mid-plane), see text in 2.3.2.1 on page 8.

ELEMENTAL COMPOSITION OF Pb-17Li

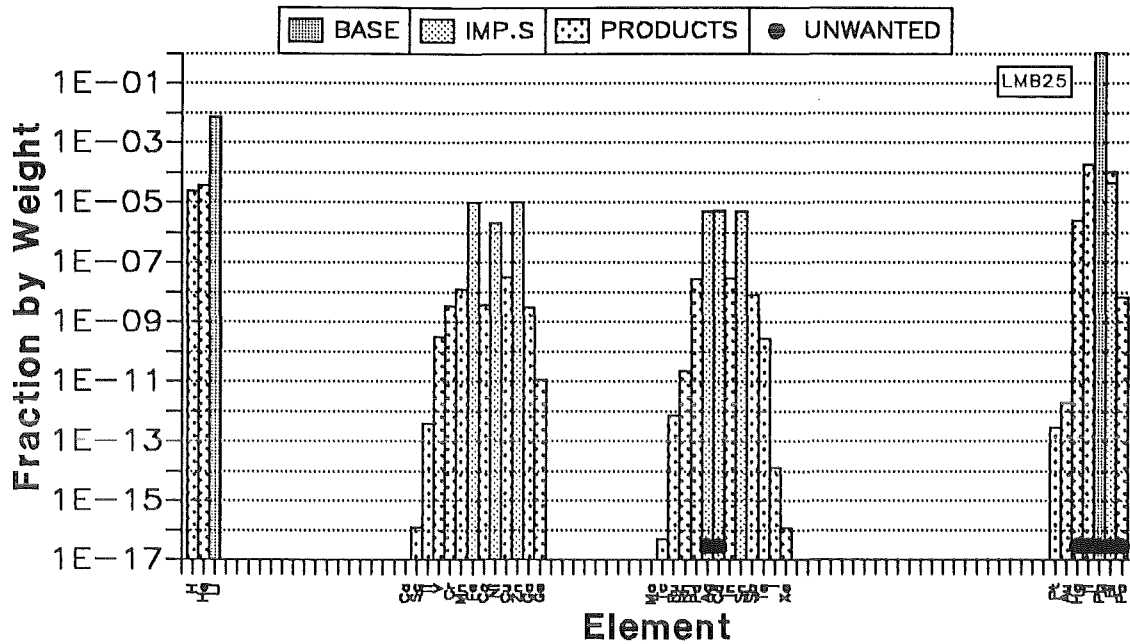


Figure 9. Elemental composition of Pb-17Li in outboard front channels. Bars give the elemental composition by weight of the liquid metal after 20000 hours of operation (ignoring circulation). Bars marked as BASE are basic constituents. IMP.S are assumed impurities. PRODUCTS are generated during irradiation. UNWANTED are activity and γ -dose rate dominating elements, see text in 2.3.1 on page 7. (Data from [4], file IRS211.FISPOU.IRSPBLI)

ELEMENTAL COMPOSITION OF MANET IN FW

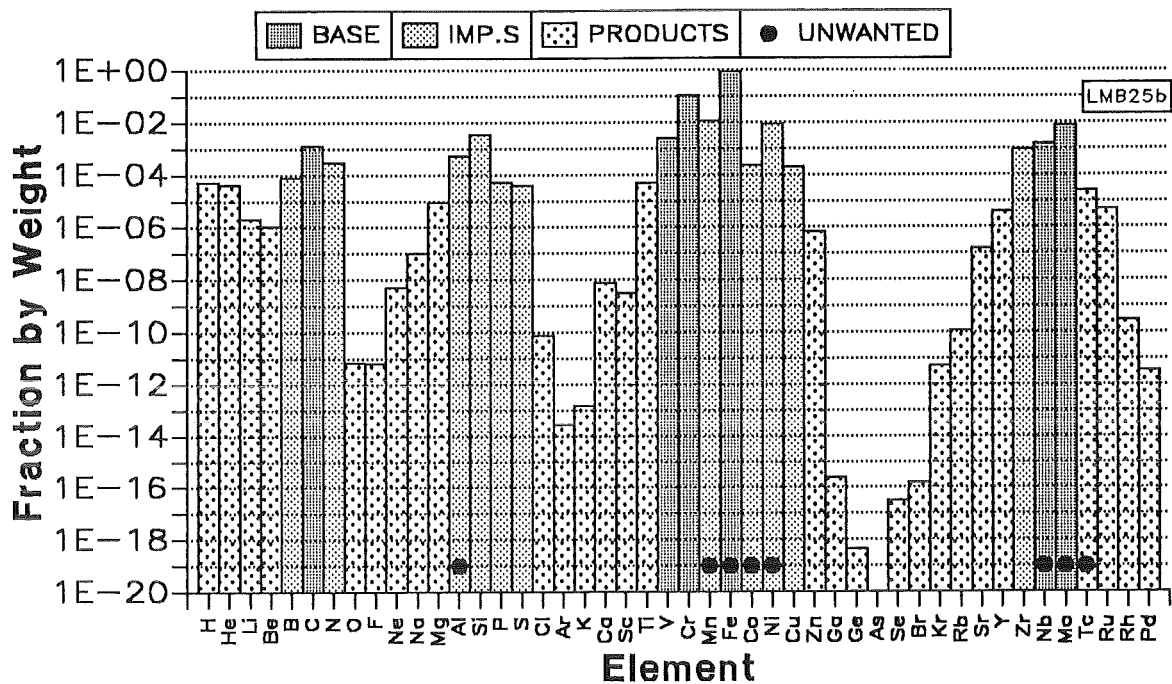


Figure 10. Elemental composition of MANET in the first wall. Bars give the elemental composition by weight of MANET after 20,000 hours of operation. Bars marked as BASE are the basic alloying elements. IMP.S are assumed impurities. PRODUCTS are generated during irradiation. UNWANTED are activity and γ -dose rate dominating elements, see text in 2.3.2.2 on page 9.

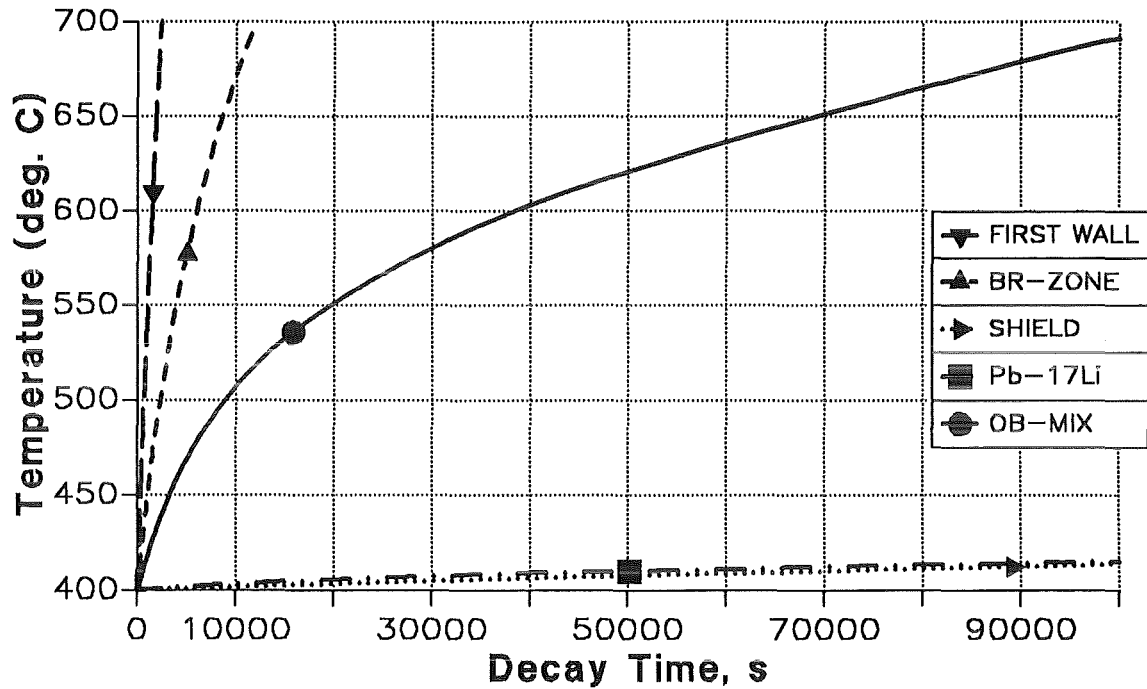


Figure 11. Adiabatic temperature rise of blanket materials due to decay heat. Curves relate to isolated materials in the first wall (MANET), breeding region (MANET or Pb-17Li), and shield region (MANET), and to a mixture of all materials in the entire outboard blanket, see text in 3.3 on page 13.

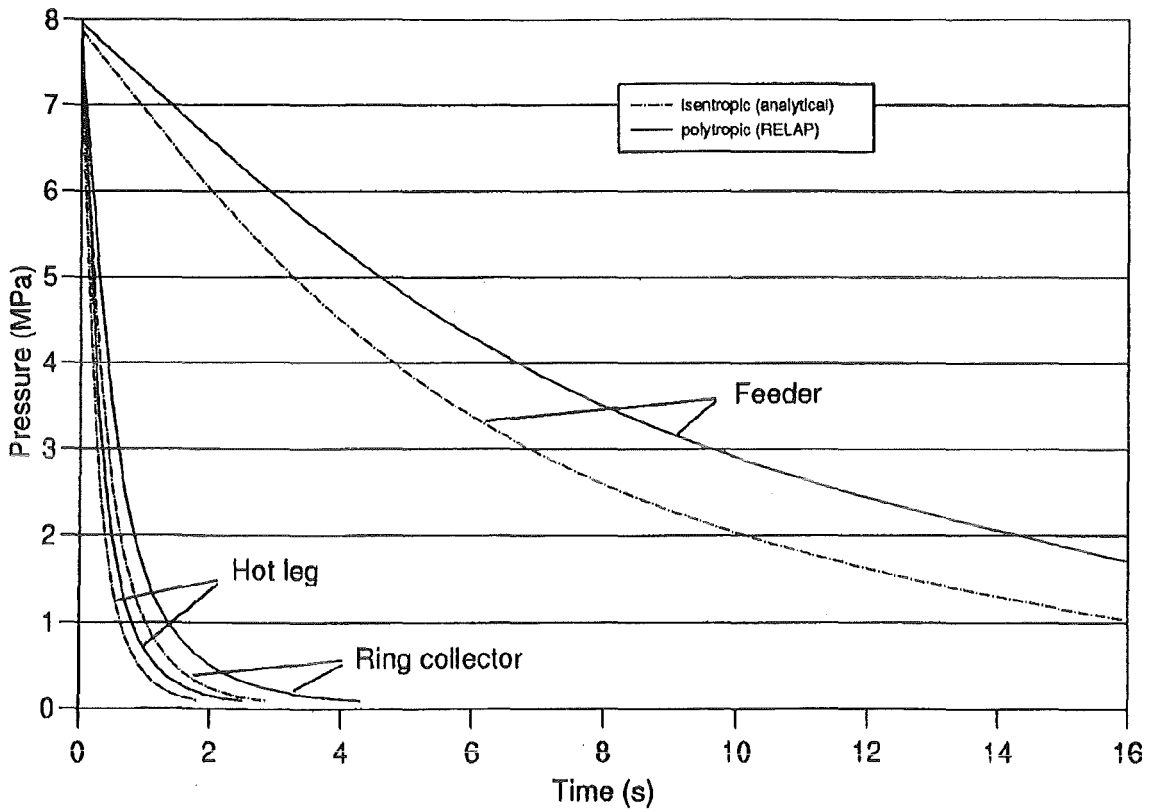


Figure 12. Depressurization of an outboard cooling subsystems. Curves refer to a double-ended helium pipe break in either the hot leg (760 mm), ring collector (600 mm), or in the feeder (150 mm), see text in 3.4 on page 15.

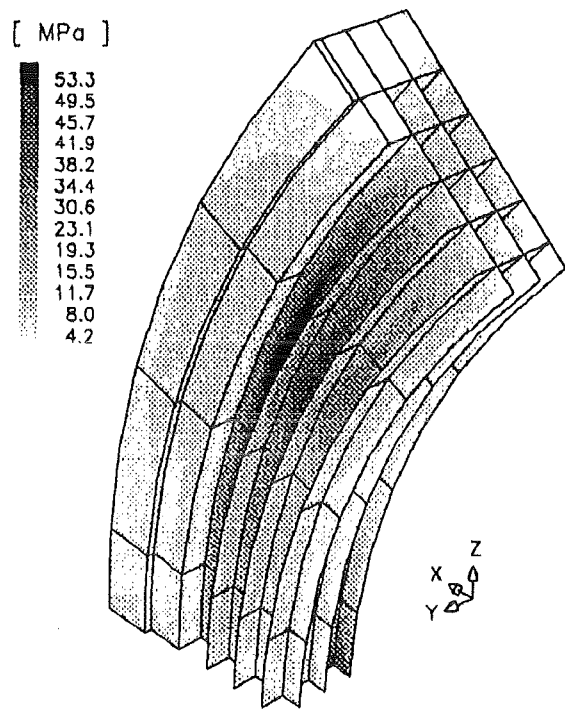


Figure 13. Distribution of von-Mises stresses with fixed back plate during a disruption.
 (One quarter model, assuming symmetry in the $y=0$ plane and in the $z=0$ plane), see text in 4.1 on page 19.

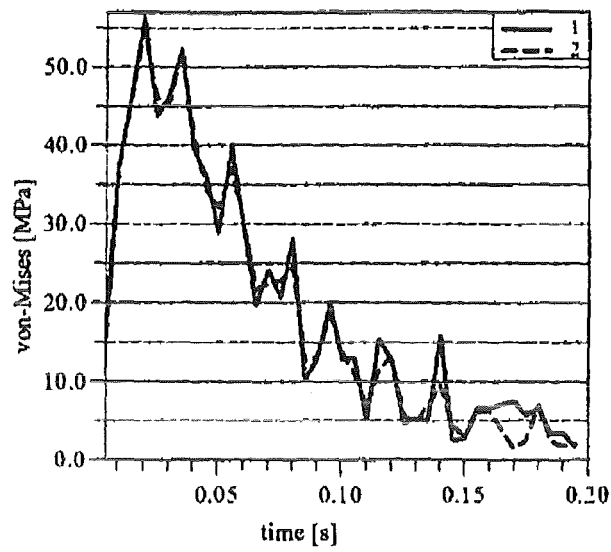


Figure 14. Maximum von-Mises stress with fixed back plate during a disruption. (1 = without, 2 = with current damping, see text in 4.1 on page 19).

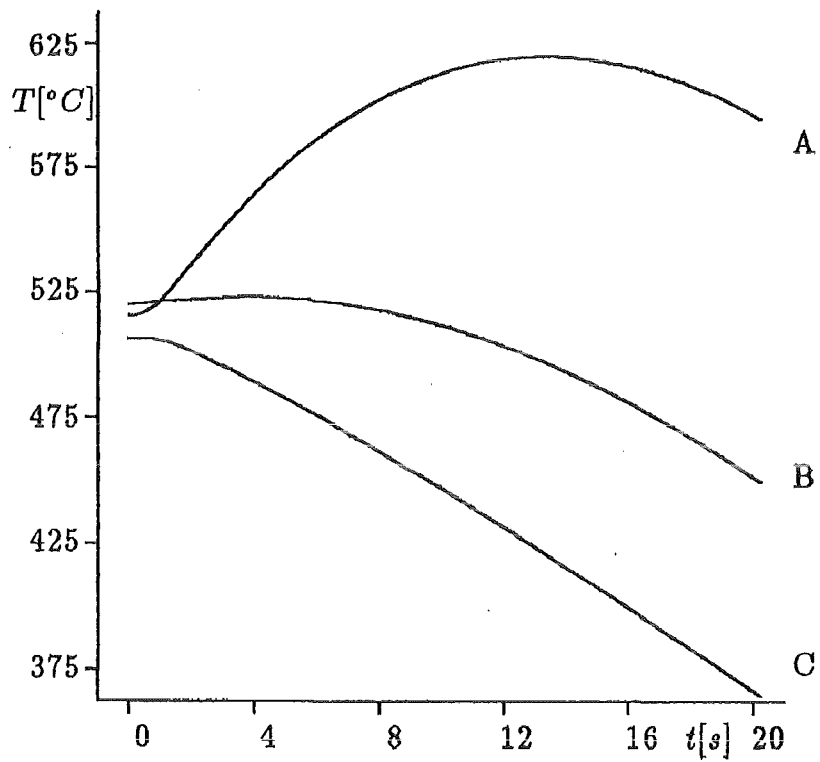


Figure 15. Temperature history during a LOCA at selected points of the first wall. Curves A, B, and C refer to points at the first wall plasma facing surface with A= at the failed channel, B= at the rib, and C= at the intact channel (see text in 4.2.1 on page 20).

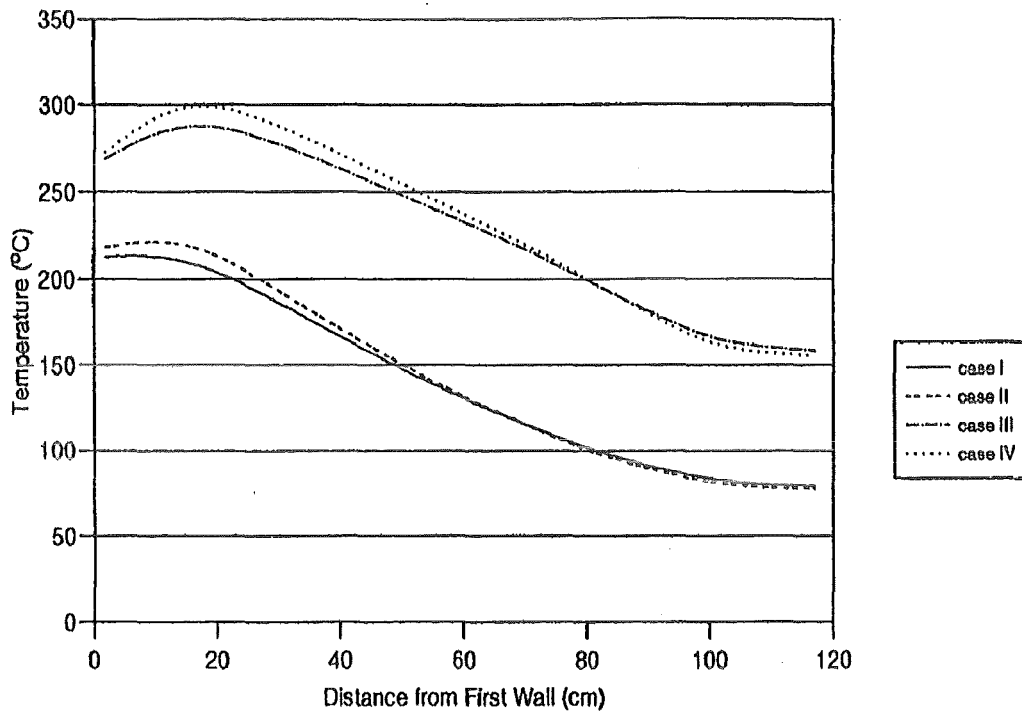


Figure 16. Radial temperature profiles in the structure of the outboard blanket segment during handling. Curves refer to the radial-poloidal midplane of the segment at steady state conditions for cases I to IV (see text in 4.3.1 on page 21).

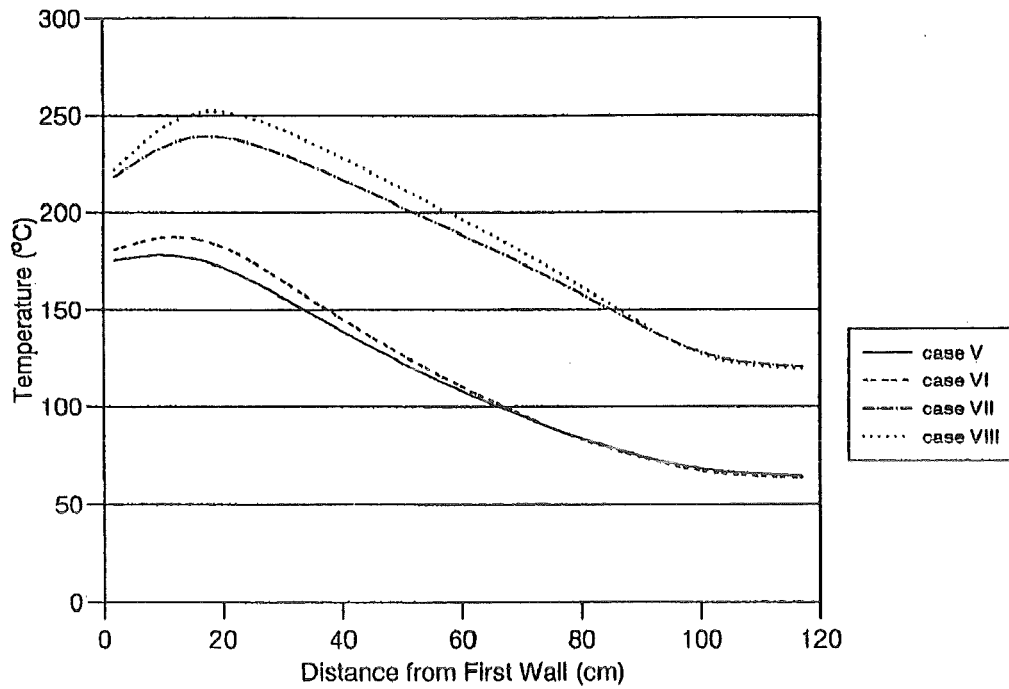


Figure 17. Radial temperature profiles in the structure of the outboard blanket segment during handling. Curves refer to the radial-poloidal midplane of the segment at steady state conditions for cases V to VIII (see text in 4.3.1 on page 21).

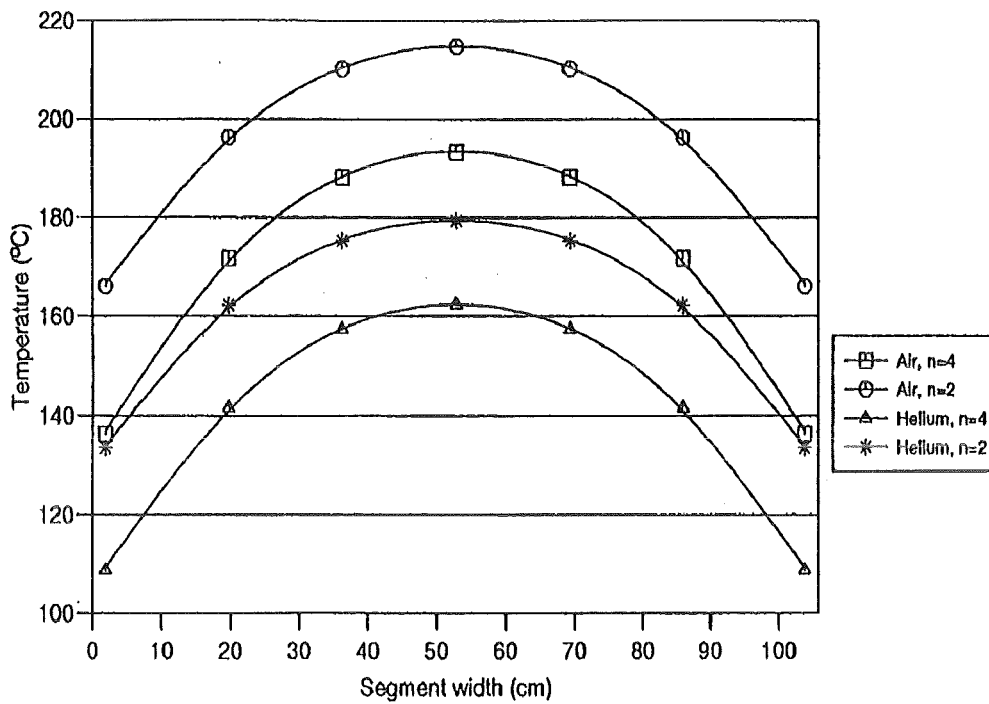
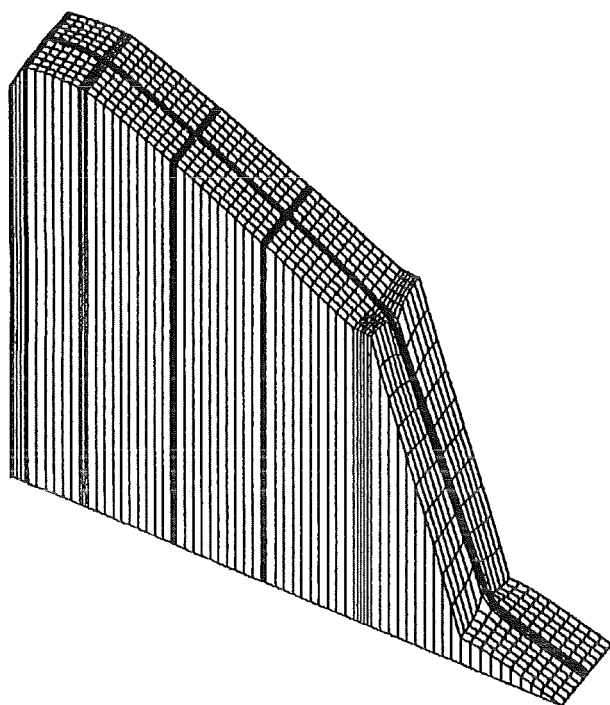


Figure 18. Toroidal temperature profiles in the structure of the outboard blanket segment during handling. Curves refer to the poloidal-toroidal sectional view through the center of the first ($n=2$) and second ($n=4$) channel row. Segment is filled with air (case I) or helium (case V), see text in 4.3.1 on page 21.



FUNCTION VALUE

MAXIMUM
0.2931E+03

MINIMUM
0.1853E+03

SURFACE VIEW

BOI 0.100E+00
HGT 0.100E+01
ANG 0.300E+03
ELV 0.450E+02

FIDAP 6.00
9/28/95
11:22:29

Figure 19. Temperature distribution in the outboard blanket segment during handling. The profile refers to the outboard segment midplane and represents a radial-poloidal slice comprising the central rib and half of the Pb-17Li channels (or helium channels and back plate) to both sides. The peak temperature is 293 °C and the minimum temperature at the back plate is 185 °C. The side walls of the slice are assumed to be adiabatic (see text in 4.3.2 on page 23).

Appendix A. Volumes and Volume Fractions

The total volume in different parts of the dual coolant blanket (outboard central and top part, and inboard central, top, and bottom part) and the volume fractions of steel, Pb-17Li, helium, and void have been calculated with specifically developed routines (LMBIN and LMBOUT) by use of the numerically problem solving tool SPEAKEASY [31]. The basis for the assessment is the vertical cross section for the DEMO reactor as shown in Figure 1 on page 54 and the midplane cross sections of outboard and inboard blanket segments taken from [6] (Figure 2 on page 55 and Figure 3 on page 56).

The main dimensions used are tabulated in Table 19.

Table 19. Main dimensions of the DEMO blanket	
Item	Length (cm)
Outboard Blanket	
Major radius to first wall at midplane of central part	827.4
Radius of curvature (poloidally) of first wall of central part	475
Poloidal angle of first wall meridian relative to midplane (deg.)	-52 to +48
Radius of curvature (toroidally) of first wall of top part	650
Length of top part	240
Depth coordinates of material layers from first wall (see A.2 on page 80)	variable D
Radial thickness of material layers (see A.2 on page 80)	variable DXI2S
Inboard Blanket	
Radius of first wall of central part at midplane	430
Length of central part	800
Length of top part (45 degrees inclined, behind divertor)	250
Length of bottom part (-45 degrees inclined, behind divertor)	250
Depth coordinates of material layers from first wall (see A.2 on page 80)	variable D
Radial thickness of material layers (see A.2 on page 80)	variable DXI2S

A.1 Results

The computed volumes for the blanket sections (outboard central part with upper extension, and inboard central part with top and bottom extensions behind the divertors) are listed in Table 20 on page 74. The total blanket volume results to $1020 m^3$ with volume fractions of 40/41/16/3 percent for steel/Pb-17Li/He/void, respectively.

Figure 20 on page 76 and Figure 21 on page 77 show the radial volume distribution of steel and Pb-17Li, respectively, for the outboard blanket (more precisely, for the central part of the outboard between the poloidal angles $\phi = -52^\circ$ to

$\phi = +48^\circ$ ¹. One can see that most of the steel is located in the back of the blanket with only 3 % of the total steel volume being in the first wall region (i.e., the first 3 radial layers). From Figure 21 on page 77 it follows that the Pb-17Li volume contained in the first channel row (next to the first wall with upward flow) amounts to 16 % of the total Pb-17Li volume in that same blanket part.

Similarly, Figure 22 on page 78 and Figure 23 on page 79 represent the radial volume distribution of steel and Pb-17Li for the inboard blanket (more precisely, for the cylindrical part of the inboard blanket with a total length of 800 cm). Again, the fraction of steel in the first wall (first three radial layers) is 3 % of the total steel volume in that part, but the fraction of Pb-17Li in the first channel row is now 34 %.

A more detailed list of the steel volume in the first wall and of the Pb-17Li volume in the first channel row for the different blanket parts is given in Table 22 on page 75.

Table 20. Volume of the dual coolant blanket. (in m ³)				
Blanket Part	Steel	Pb-17Li	Helium	Void
Outboard central part	199	269	112	13
Outboard top part	44	59	24	4
Outboard total	243	328	136	17
Inboard central part	90	52	16	8
inboard top part	36	20	6	3
inboard bottom part	36	20	6	3
Inboard total	162	92	28	14
Outboard + Inboard total	405	420	164	31
Total blanket volume	1020			

¹ Note that this is not identical to the assumption $\phi = \pm 45^\circ$ made in the neutronics analyses which leads to lower volumes, in total for the outboard central part of 8.7 %.

Table 21. Volume fractions of steel and Pb-17Li in different blanket parts. Volumes are given in (m^3) and in percent of the total material volume in the respective blanket part.

Blanket Part	Steel volume in first wall		Pb-17Li volume in first channel row	
	(m^3)	(%)	(m^3)	(%)
Outboard central part	5.98	3.0	41.7	15.5
Outboard top part	1.508	3.4	9.6	16.2
Outboard total	7.4	3.04	51.3	15.6
Inboard central part	2.88	3.18	17.6	33.8
inboard top part	1.09	3.0	6.7	33.4
inboard bottom part	1.09	3.0	6.7	33.4
Inboard total	5.05	3.1	31.0	33.6
Outboard + Inboard total	12.452	3.06	82.3	19.6

Table 22. Steel volumes in the different blanket parts. Values are in m^3 . Multiply by the density for MANET of $7700 \text{ kg}/m^3$ to obtain masses.

Blanket Part	First Wall (first 3 layers)	Breeding Zone	Shield Region	Total FW + BZ + SH
Outboard central part	5.98	82.7	109.8	198.5
Outboard top part	1.508	20.3	22.5	44.3
Outboard total	7.488	103	132.3	242.8
Inboard central part	2.88	33.1	54.3	90.3
inboard top part	1.09	13.0	22.1	36.1
inboard bottom part	1.09	13.0	22.1	36.1
inboard total	5.05	59.0	98.5	162.6
IB + OB total	12.5	162.0	230.8	405.4

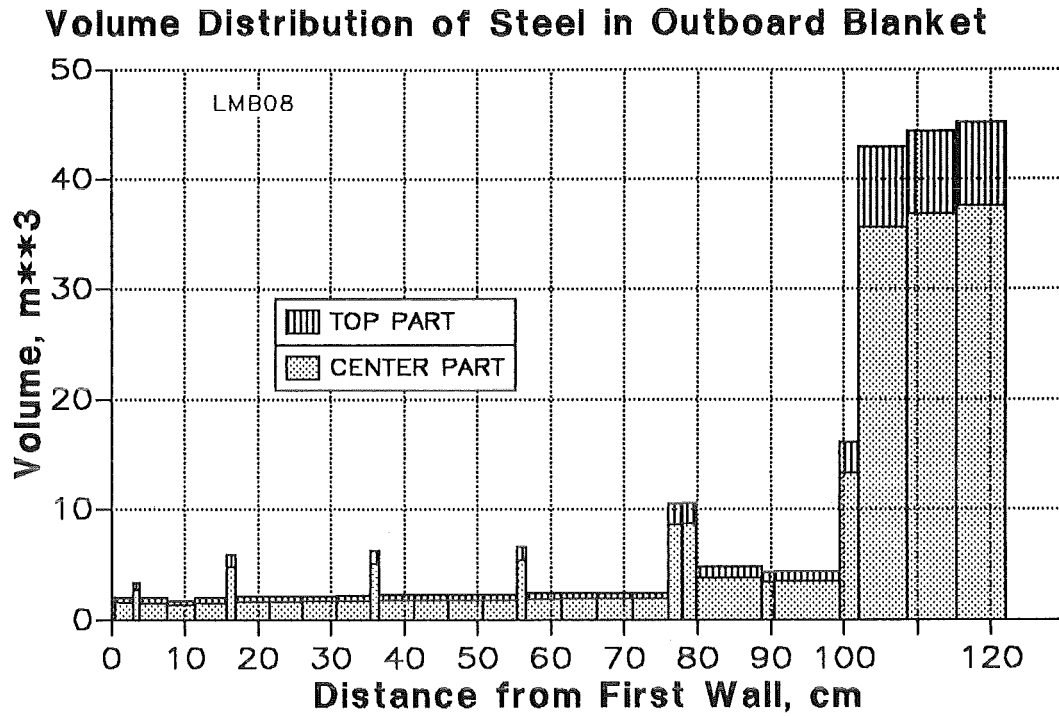


Figure 20. Volume histogram of steel for radial layers in the outboard blanket. Bar heights give the steel volume in the respective layers. The diagram refers to the outboard center part between poloidal angles of -52 to +48 degree and to the top part. The total steel volume is 243 m^3 ($1.87 \times 10^6 \text{ kg}$), i.e., 39000 kg per outboard segment.

Volume Distribution of Pb-17Li in Outboard Blanket

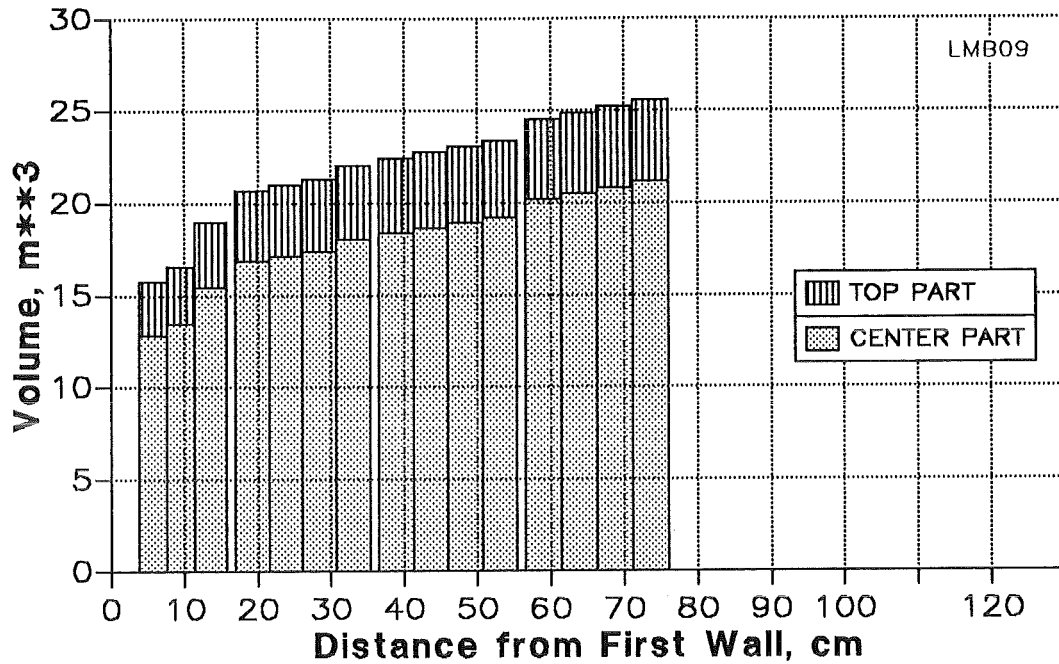


Figure 21. Volume histogram of Pb-17Li for radial layers in the outboard blanket. Bar heights give the Pb-17Li volume in the respective layers. The diagram refers to the outboard center part between poloidal angles of -52 to +48 degree and to the top part. The total Pb-17Li volume is 328 m^3 ($3.05 \times 10^6 \text{ kg}$), i.e., 63000 kg per outboard segment.

Volume Distribution of Steel in Inboard Blanket

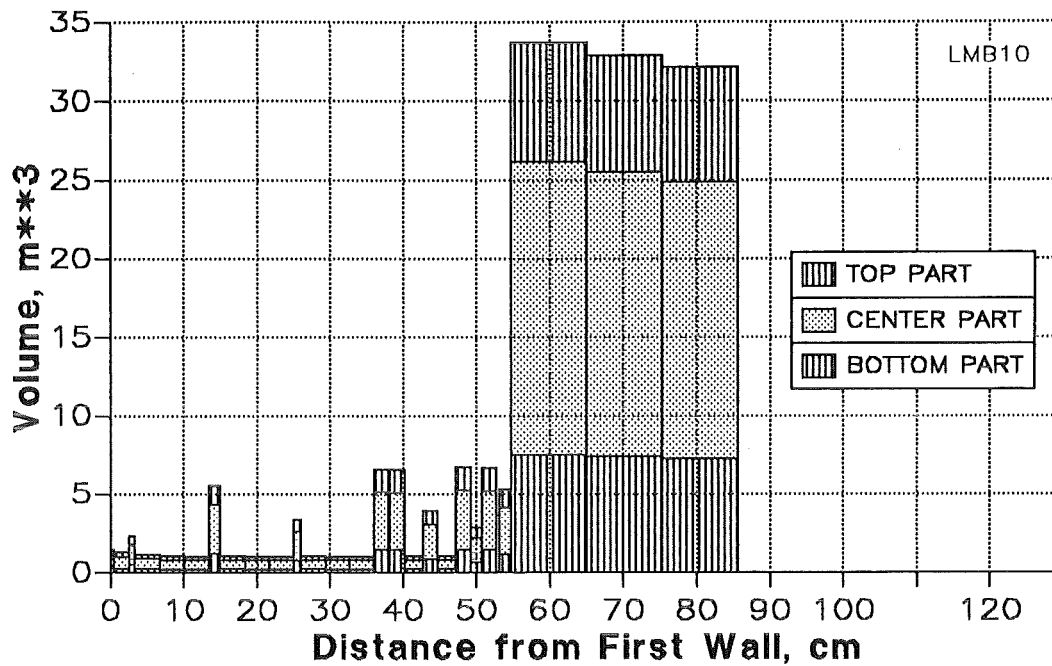


Figure 22. Volume histogram of steel for radial layers in the inboard blanket. Bar heights give the steel volume in the respective layers. The diagram refers to the inboard center part with a height of 800 cm and to the top and bottom part with a length of 250 cm. The total steel volume is 162 m^3 ($1.25 \times 10^6 \text{ kg}$), i.e., 39000 kg per inboard segment.

Volume Distribution of Pb-17Li in Inboard Blanket

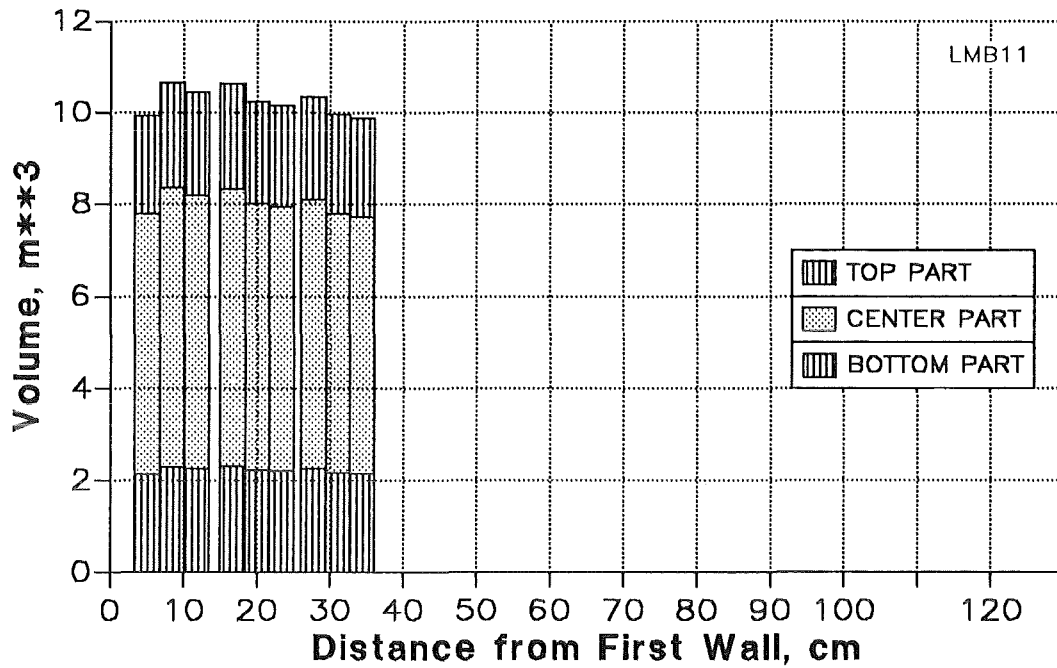


Figure 23. Volume histogram of Pb-17Li for radial layers in the inboard blanket. Bar heights give the Pb-17Li volume in the respective layers. The diagram refers to the inboard center part with a height of 800 cm and to the top and bottom part with a length of 250 cm. The total Pb-17Li volume is 92 m^3 ($0.856 \times 10^6 \text{ kg}$), i.e., 26700 kg per inboard segment.

A.2 Detailed Results

The following tables give the computer output for individual radial material layers assuming a 100 % toroidal coverage. The volumes for each radial layer in the respective blanket part pertaining to steel/Pb-17Li/helium/void are listed in the four columns of the array VIJ. Corresponding volume fractions are represented by the array MATVEC. The variables are defined as follows:

Table 23. Definition of variables used in Appendix A		
Variable	Unit	Definition
AI	cm^2	Mean surface of radial layer
AL	degrees	Angle of first wall meridian relative to torus axis
D	cm	Radial depth from first wall of radial layer surface
DXI2S	cm	Thickness of radial layer
E	cm	Eccentricity (radius of first wall at midplane minus RFW)
HEA	cm	Toroidal width of helium in radial layer per segment
L	cm	Length of blanket part
MATVEC	1	Volume fractions of steel/Pb-17Li/helium/void (columns) in radial layers (rows)
PBLIA	cm	Toroidal width of Pb-17Li in radial layer per segment
RFW	cm	Radius of curvature of first wall (poloidally)
STEELA	cm	Toroidal width of steel in radial layer per segment
SUM-COLS (VIJ)	cm^3	Sum over all layers of volumes of steel/Pb-17Li/helium/void
V	cm^3	Total volume of blanket part
VI	cm^3	Total volume of radial layer
VIJ	cm^3	Volumes of steel/Pb-17Li/helium/void (columns) in radial layers (rows)
VOIDA	cm	Toroidal width of void in radial layer per segment
WIDTH	cm	Mean toroidal width of radial layer per segment at midplane
X0	cm	Radius of first wall relative to torus axis
XI2S	cm	Radial depth coordinate of center of radial layer

A.2.1 Outboard Blanket (central part)

RFW	E	D	XI2S	DXI2S	AI	VI	D	XI2S	DXI2S	MATVEC			
***	*****	*****	*****	*****	*****	*****	*****	*****	*****	*****	*****	*****	
475	352.4	0	.25	.5	4009295	2004647	0	.25	.5	.84032	0	0	.15968
		.5	1.75	2.5	4028842	10072106	.5	1.75	2.5	.15387	0	.754	.092136
		3	3.4	.8	4050366	3240293	3	3.4	.8	.84828	0	.087355	.064367
		3.8	5.7	3.8	4080507	15505928	3.8	5.7	3.8	.098118	.82669	.038514	.03668
		7.6	9.5	3.8	4130475	15695803	7.6	9.5	3.8	.085806	.8576	.038339	.018257
		11.4	13.55	4.3	4184045	17991392	11.4	13.55	4.3	.085392	.85828	.038154	.018169
		15.7	16.3	1.2	4220552	5064662	15.7	16.3	1.2	.94386	0	.03803	.018109
		16.9	19.2	4.6	4259298	19592772	16.9	19.2	4.6	.084823	.85923	.037899	.018047
		21.5	23.8	4.6	4321015	19876670	21.5	23.8	4.6	.084364	.85999	.037695	.01795
		26.1	28.4	4.6	4383139	20162440	26.1	28.4	4.6	.083911	.86074	.037492	.017853
		30.7	33.05	4.7	4446354	20897865	30.7	33.05	4.7	.083457	.8615	.037289	.017757
		35.4	36	1.2	4486623	5383948	35.4	36	1.2	.94514	0	.037162	.017696
		36.6	38.95	4.7	4527159	21277645	36.6	38.95	4.7	.082889	.86244	.037035	.017636
		41.3	43.65	4.7	4592007	21582435	41.3	43.65	4.7	.082442	.86318	.036836	.017541
		46	48.35	4.7	4657281	21889222	46	48.35	4.7	.081999	.86392	.036638	.017447
		50.7	53.05	4.7	4722980	22198007	50.7	53.05	4.7	.081561	.86464	.036442	.017353
		55.4	56	1.2	4764384	5717261	55.4	56	1.2	.94638	0	.036321	.017296
		56.6	59.025	4.85	4807119	23314525	56.6	59.025	4.85	.081012	.86556	.036197	.017237
		61.45	63.875	4.85	4875917	23648199	61.45	63.875	4.85	.080571	.86629	.036	.017143
		66.3	68.725	4.85	4945169	23984067	66.3	68.725	4.85	.080135	.86701	.035805	.01705
		71.15	73.575	4.85	5014872	24322131	71.15	73.575	4.85	.079703	.86773	.035612	.016958
		76	76.9	1.8	5062872	9113169	76	76.9	1.8	.94762	0	.035481	.016896
		77.8	77.9	.2	5077356	1015471	77.8	77.9	.2	.079323	0	.035442	.88524
		78	78.9	1.8	5091875	9165375	78	78.9	1.8	.94774	0	.035403	.016859
		79.8	84.3	9	5170756	46536806	79.8	84.3	9	.082118	0	.90112	.016759
		88.8	89.65	1.7	5249087	8923448	88.8	89.65	1.7	.38487	0	.59847	.016661
		90.5	95	9	5328344	47955097	90.5	95	9	.072883	0	.91055	.016564
		99.5	100.75	2.5	5413759	13534398	99.5	100.75	2.5	.98354	0	0	.016462
		102	105.3	6.6	5482032	36181408	102	105.3	6.6	.98198	0	0	.018019
		108.6	111.95	6.7	5582402	37402097	108.6	111.95	6.7	.98373	0	0	.016265
		115.3	118.65	6.7	5684385	38085382	115.3	118.65	6.7	.98385	0	0	.01615

XI2S	WIDTH	STEELA	PBLIA	HEA	VOIDA
*****	*****	*****	*****	*****	*****
.25	108.34	91.039	0	0	17.3
1.75	108.54	16.7	0	81.835	10
3.4	108.75	92.251	0	9.5	7
5.7	109.05	10.7	90.152	4.2	4
9.5	109.55	9.4	93.95	4.2	2
13.55	110.08	9.4	94.48	4.2	2
16.3	110.44	104.24	0	4.2	2
19.2	110.82	9.4	95.22	4.2	2
23.8	111.42	9.4	95.822	4.2	2
28.4	112.02	9.4	96.424	4.2	2
33.05	112.63	9.4	97.033	4.2	2
36	113.02	106.82	0	4.2	2
38.95	113.4	9.4	97.805	4.2	2
43.65	114.02	9.4	98.42	4.2	2
48.35	114.64	9.4	99.035	4.2	2
53.05	115.25	9.4	99.651	4.2	2
56	115.64	109.44	0	4.2	2
59.025	116.03	9.4	100.43	4.2	2
63.875	116.67	9.4	101.07	4.2	2
68.725	117.3	9.4	101.7	4.2	2
73.575	117.94	9.4	102.34	4.2	2
76.9	118.37	112.17	0	4.2	2
77.9	118.5	9.4	0	4.2	104.9
78.9	118.63	112.43	0	4.2	2
84.3	119.34	9.8	0	107.54	2
89.65	120.04	46.2	0	71.841	2
95	120.74	8.8	0	109.94	2
100.75	121.49	119.49	0	0	2
105.3	122.09	119.89	0	0	2
111.95	122.96	120.96	0	0	2
118.65	123.84	121.84	0	0	2

XI2S	DXI2S	VIj		
*****	*****	*****	*****	*****
.25	.5	1684537	0	0 320110
1.75	2.5	1549763	0	7594341 928002
3.4	.8	2748668	0	283056 208568
5.7	3.8	1521410	12818578	597189 568751
9.5	3.8	1346789	13460707	601757 286551
13.55	4.3	1536329	15441740	686445 326878
16.3	1.2	4780337	0	192608 91718
19.2	4.6	1661909	16834711	742555 353598
23.8	4.6	1676878	17093765	749244 356783
28.4	4.6	1691844	17354698	755930 359967
33.05	4.7	1744078	18003438	779269 371080
36	1.2	5088594	0	200078 95275
38.95	4.7	1763680	18350687	788027 375251
43.65	4.7	1779291	18629569	795002 378573
48.35	4.7	1794898	18910455	801976 381893
53.05	4.7	1810501	19193345	808947 385213
56	1.2	5410723	0	207655 98883
59.025	4.85	1888749	20180006	843909 401861
63.875	4.85	1905355	20486120	851329 405395
68.725	4.85	1921958	20794435	858747 408927
73.575	4.85	1938557	21104952	866164 412459
76.9	1.8	8635848	0	323346 153974
77.9	.2	80550	0	35990 898931
78.9	1.8	8686380	0	324481 154515
84.3	9	3821487	0	41935423 779895
89.65	1.7	3434341	0	5340434 148673
95	9	3495102	0	43665653 794341
100.75	2.5	13311600	0	0 222799
105.3	6.6	35529437	0	0 651970
111.95	6.7	36793737	0	0 608359
118.65	6.7	37470296	0	0 615086

V	SUM(VIJ)	SUMCOLS(VIJ)	PERCENT
*****	*****	*****	*****
5.9133E8	5.9133E8	1.985E8	.33569
		2.6866E8	.45432
		1.1163E8	.18878
		12544281	.021214

A.2.2 Outboard Blanket (top part)

X0	L	D	AL	XI2S	DXI2S	AI	VI	D	XI2S	DXI2S	MATVEC
***	***	*****	**	*****	*****	*****	*****	*****	*****	*****	*****
650	240	0	0	.25	.5	980553	490277	0	.25	.5	.79675 0 0 .20325
		.5		1.75	2.5	982815	2457038	.5	1.75	2.5	.19575 0 .68704 .11721
		3		3.4	.8	985303	788243	3	3.4	.8	.80708 0 .11107 .081843
		3.8		5.7	3.8	988771	3757332	3.8	5.7	3.8	.12466 .7798 .048933 .046603
		7.6		9.5	3.8	994502	3779107	7.6	9.5	3.8	.10889 .81929 .048651 .023167
		11.4		13.55	4.3	1000609	4302619	11.4	13.55	4.3	.10822 .8204 .048355 .023026
		15.7		16.3	1.2	1004756	1205707	15.7	16.3	1.2	.92891 0 .048155 .022931
		16.9		19.2	4.6	1009129	4641993	16.9	19.2	4.6	.10731 .82191 .047946 .022832
		21.5		23.8	4.6	1016066	4673902	21.5	23.8	4.6	.10658 .82313 .047619 .022676
		26.1		28.4	4.6	1023002	4705810	26.1	28.4	4.6	.10585 .82433 .047296 .022522
		30.7		33.05	4.7	1030014	4841067	30.7	33.05	4.7	.10513 .82552 .046974 .022369
		35.4		36	1.2	1034463	1241355	35.4	36	1.2	.93096 0 .046772 .022272
		36.6		38.95	4.7	1038911	4882883	36.6	38.95	4.7	.10423 .82702 .046572 .022177
		41.3		43.65	4.7	1045999	4916194	41.3	43.65	4.7	.10353 .82819 .046256 .022027
		46		48.35	4.7	1053086	4949505	46	48.35	4.7	.10283 .82935 .045945 .021879
		50.7		53.05	4.7	1060174	4982816	50.7	53.05	4.7	.10214 .83049 .045638 .021732
		55.4		56	1.2	1064622	1277546	55.4	56	1.2	.93291 0 .045447 .021641
		56.6		59.025	4.85	1069184	5185540	56.6	59.025	4.85	.10128 .83192 .045253 .021549
		61.45		63.875	4.85	1076497	5221012	61.45	63.875	4.85	.10059 .83306 .044946 .021403
		66.3		68.725	4.85	1083811	5256483	66.3	68.725	4.85	.099914 .83419 .044642 .021258
		71.15		73.575	4.85	1091124	5291954	71.15	73.575	4.85	.099244 .8353 .044343 .021116
		76		76.9	1.8	1096138	1973049	76	76.9	1.8	.93484 0 .04414 .021019
		77.8		77.9	.2	1097646	219529	77.8	77.9	.2	.098655 0 .04408 .85727
		78		78.9	1.8	1099154	1978478	78	78.9	1.8	.93502 0 .044019 .020962
		79.8		84.3	9	1107297	9965676	79.8	84.3	9	.10196 0 .87724 .020807
		88.8		89.65	1.7	1115365	1896120	88.8	89.65	1.7	.47717 0 .50217 .020657
		90.5		95	9	1123433	10110893	90.5	95	9	.090238 0 .88925 .020509
		99.5		100.75	2.5	1132103	2830258	99.5	100.75	2.5	.97965 0 0 .020351
		102		105.3	6.6	1138965	7517166	102	105.3	6.6	.97775 0 0 .022252
		108.6		111.95	6.7	1148993	7698250	108.6	111.95	6.7	.97995 0 0 .020052
		115.3		118.65	6.7	1159096	7765943	115.3	118.65	6.7	.98012 0 0 .019878
		122						122			

XI2S	WIDTH	STEELA	PBLIA	HEA	VOIDA	XI2S	DXI2S	VIJ
*****	*****	*****	*****	*****	****	*****	*****	*****
.25	85.117	67.817	0	0	17.3	.25	.5	390629 0 0 99648
1.75	85.314	16.7	0	58.614	10	1.75	2.5	480960 0 1688078 288000
3.4	85.53	69.03	0	9.5	7	3.4	.8	636179 0 87552 64512
5.7	85.831	10.7	66.931	4.2	4	5.7	3.8	468403 2929965 183859 175104
9.5	86.328	9.4	70.728	4.2	2	9.5	3.8	411494 3096201 183859 87552
13.55	86.858	9.4	71.258	4.2	2	13.55	4.3	465638 3529857 208051 99072
16.3	87.218	81.018	0	4.2	2	16.3	1.2	1119998 0 58061 27648
19.2	87.598	9.4	71.998	4.2	2	19.2	4.6	498125 3815318 222566 105984
23.8	88.2	9.4	72.6	4.2	2	23.8	4.6	498125 3847227 222566 105984
28.4	88.802	9.4	73.202	4.2	2	28.4	4.6	498125 3879135 222566 105984
33.05	89.411	9.4	73.811	4.2	2	33.05	4.7	508954 3996421 227405 108288
36	89.797	83.597	0	4.2	2	36	1.2	1155647 0 58061 27648
38.95	90.183	9.4	74.583	4.2	2	38.95	4.7	508954 4038236 227405 108288
43.65	90.798	9.4	75.198	4.2	2	43.65	4.7	508954 4071547 227405 108288
48.35	91.414	9.4	75.814	4.2	2	48.35	4.7	508954 4104858 227405 108288
53.05	92.029	9.4	76.429	4.2	2	53.05	4.7	508954 4138169 227405 108288
56	92.415	86.215	0	4.2	2	56	1.2	1191838 0 58061 27648
59.025	92.811	9.4	77.211	4.2	2	59.025	4.85	525197 4313937 234662 111744
63.875	93.446	9.4	77.846	4.2	2	63.875	4.85	525197 4349408 234662 111744
68.725	94.081	9.4	78.481	4.2	2	68.725	4.85	525197 4384879 234662 111744
73.575	94.716	9.4	79.116	4.2	2	73.575	4.85	525197 4420350 234662 111744
76.9	95.151	88.951	0	4.2	2	76.9	1.8	1844486 0 87091 41472
77.9	95.282	9.4	0	4.2	81.682	77.9	.2	21658 0 9676.8 188195
78.9	95.413	89.213	0	4.2	2	78.9	1.8	1849915 0 87091 41472
84.3	96.12	9.8	0	84.32	2	84.3	9	1016064 0 8742252 207360
89.65	96.82	46.2	0	48.62	2	89.65	1.7	904781 0 952172 39168
95	97.52	8.8	0	86.72	2	95	9	912384 0 8991149 207360
100.75	98.273	96.273	0	0	2	100.75	2.5	2772658 0 0 57600
105.3	98.868	96.668	0	0	2.2	105.3	6.6	7349896 0 0 167270
111.95	99.739	97.739	0	0	2	111.95	6.7	7543882 0 0 154368
118.65	100.62	98.616	0	0	2	118.65	6.7	7611575 0 0 154368
V	SUM(VIJ)	SUMCOLS(VIJ)	PERCENT					
1.308E8	1.308E8	44288013	.33858					
		58915510	.45041					
		24138387	.18454					
		3461833	.026466					

A.2.3 Inboard Blanket (central part)

X0	L	D	AL	XI2S	DXI2S	AI	VI	D	XI2S	DXI2S	MATVEC
***	***	*****	**	*****	*****	*****	*****	*****	*****	*****	*****
430	800	0	0	-.25	.5	2160157	1080079	0	-.25	.5	.76891 0 0 .23109
		-5		-1.5	2	2153874	4307748	-.5	-1.5	2	.16996 0 .67552 .15451
		-2.5		-2.9	.8	2146837	1717470	-2.5	-2.9	.8	.76747 0 .11328 .11925
		-3.3		-5	3.4	2136281	7263356	-3.3	-5	3.4	.089876 .77711 .053925 .079091
		-6.7		-8.4	3.4	2119191	7205249	-6.7	-8.4	3.4	.082145 .83933 .039864 .038656
		-10.1		-11.75	3.3	2102352	6937762	-10.1	-11.75	3.3	.082802 .85266 .040184 .024354
		-13.4		-14.2	1.6	2090037	3344059	-13.4	-14.2	1.6	.93508 0 .04042 .024497
		-15		-16.7	3.4	2077471	7063400	-15	-16.7	3.4	.083794 .8509 .040665 .024645
		-18.4		-20.05	3.3	2060632	6800085	-18.4	-20.05	3.3	.084479 .84968 .040997 .024847
		-21.7		-23.35	3.3	2044044	6745346	-21.7	-23.35	3.3	.085165 .84846 .04133 .025048
		-25		-25.5	1	2033237	2033237	-25	-25.5	1	.93327 0 .04155 .025182
		-26		-27.7	3.4	2022179	6875407	-26	-27.7	3.4	.086085 .84682 .041777 .025319
		-29.4		-31.05	3.3	2005340	6617621	-29.4	-31.05	3.3	.086808 .84553 .042128 .025532
		-32.7		-34.35	3.3	1988752	6562882	-32.7	-34.35	3.3	.087532 .84424 .042479 .025745
		-36		-37	2	1975432	3950864	-36	-37	2	.93132 0 .042765 .025918
		-38		-38.1	.2	1969903	393981	-38	-38.1	.2	.041586 0 .042885 .91553
		-38.2		-39.2	2	1964373	3928747	-38.2	-39.2	2	.93093 0 .043006 .026064
		-40.2		-41.45	2.5	1953064	4882659	-40.2	-41.45	2.5	.12059 0 .85319 .026215
		-42.7		-43.7	2	1941754	3883508	-42.7	-43.7	2	.56823 0 .4054 .026368
		-44.7		-45.95	2.5	1930444	4826111	-44.7	-45.95	2.5	.122 0 .85147 .026522
		-47.2		-48.2	2	1919134	3838269	-47.2	-48.2	2	.97332 0 0 .026679
		-49.2		-49.95	1.5	1910338	2865507	-49.2	-49.95	1.5	.55777 0 0 .44223
		-50.7		-51.7	2	1901542	3803083	-50.7	-51.7	2	.97307 0 0 .026926
		-52.7		-52.9	.4	1895510	758204	-52.7	-52.9	.4	.044568 0 0 .95543
		-53.1		-53.9	1.6	1890483	3024773	-53.1	-53.9	1.6	.97292 0 0 .027083
		-54.7		-59.85	10.3	1860575	19163925	-54.7	-59.85	10.3	.97248 0 0 .027518
		-65		-70.15	10.3	1808802	18630659	-65	-70.15	10.3	.97169 0 0 .028306
		-75.3		-80.45	10.3	1757028	18097393	-75.3	-80.45	10.3	.97086 0 0 .02914
		-85.6						-85.6			

XI2S	WIDTH	STEELA	PBLIA	HEA	VOIDA	XI2S	DXI2S	VIJ	
*****	*****	*****	*****	*****	*****	*****	*****	*****	
-.25	84.381	64.881	0	0	19.5	-.25	.5	830479 0 0 249600	
-1.5	84.136	14.3	0	56.836	13	-1.5	2	732160 0 2909988 665600	
-2.9	83.861	64.361	0	9.5	10	-2.9	.8	1318110 0 194560 204800	
-5	83.448	7.5	64.848	4.5	6.6	-5	3.4	652800 5644412 391680 574464	
-8.4	82.781	6.8	69.481	3.3	3.2	-8.4	3.4	591872 6047617 287232 278528	
-11.75	82.123	6.8	70.023	3.3	2	-11.75	3.3	574464 5915554 278784 168960	
-14.2	81.642	76.342	0	3.3	2	-14.2	1.6	3126971 0 135168 81920	
-16.7	81.151	6.8	69.051	3.3	2	-16.7	3.4	591872 6010216 287232 174080	
-20.05	80.493	6.8	68.393	3.3	2	-20.05	3.3	574464 5777877 278784 168960	
-23.35	79.845	6.8	67.745	3.3	2	-23.35	3.3	574464 5723138 278784 168960	
-25.5	79.423	74.123	0	3.3	2	-25.5	1	1897557 0 84480 51200	
-27.7	78.991	6.8	66.891	3.3	2	-27.7	3.4	591872 5822223 287232 174080	
-31.05	78.334	6.8	66.234	3.3	2	-31.05	3.3	574464 5595413 278784 168960	
-34.35	77.686	6.8	65.586	3.3	2	-34.35	3.3	574464 5540674 278784 168960	
-37	77.165	71.865	0	3.3	2	-37	2	3679504 0 168960 102400	
-38.1	76.949	3.2	0	3.3	70.449	-38.1	.2	16384 0 16896 360701	
-39.2	76.733	71.433	0	3.3	2	-39.2	2	3657387 0 168960 102400	
-41.45	76.292	9.2	0	65.092	2	-41.45	2.5	588800 0 4165859 128000	
-43.7	75.85	43.1	0	30.75	2	-43.7	2	2206720 0 1574388 102400	
-45.95	75.408	9.2	0	64.208	2	-45.95	2.5	588800 0 4109311 128000	
-48.2	74.966	72.966	0	0	2	-48.2	2	3735869 0 0 102400	
-49.95	74.623	41.623	0	0	33	-49.95	1.5	1598307 0 0 1267200	
-51.7	74.279	72.279	0	0	2	-51.7	2	3700683 0 0 102400	
-52.9	74.043	3.3	0	0	70.743	-52.9	.4	33792 0 0 724412	
-53.9	73.847	71.847	0	0	2	-53.9	1.6	2942853 0 0 81920	
-59.85	72.679	70.679	0	0	2	-59.85	10.3	18636565 0 0 527360	
-70.15	70.656	68.656	0	0	2	-70.15	10.3	18103299 0 0 527360	
-80.45	68.634	66.634	0	0	2	-80.45	10.3	17570033 0 0 527360	
V	SUM(VI2S)	SUMCOLS(VI2S)	PERCENT			V	SUM(VI2S)	SUMCOLS(VI2S)	PERCENT
1.666E8	1.666E8	90265009	.5418			1.666E8	1.666E8	90265009	.5418
		52077124	.31259					52077124	.31259
		16175866	.097093					16175866	.097093
		8083384	.048519					8083384	.048519

